Supporting Information

Two-Photon Microprinting of 3D Emissive Structures Using Tetraazaperylene-Derived Fluorophores

Robert Eichelmann, Joël Monti, Li-Yun Hsu, Finn Kröger, Joachim Ballmann, Eva Blasco, Lutz H. Gade

Outline

1. General Information

All chemicals and solvents were purchased from commercial suppliers and used without further purification. Solvents were dried according to standard procedures. Deuterated solvents were bought from Euriso Top or Sigma–Aldrich and used as received. The ^{1}H and ^{13}C spectra were recorded with a Bruker and 600II spectrometer and are referenced to the residual signal of $CDCl_3$ (^{1}H: 7.26 ppm and ^{13}C: 77.16 ppm.[1] Chemical shifts are given in ppm and coupling constants in Hz. The following abbreviations were used to describe the multiplicities: s = singlet, m = multiplet. The mass spectra were recorded by the department of the organic Chemistry of the University of Heidelberg under the direction of Dr. J. Gross. MALDI spectra were measured on a Bruker ApexQe hybrid 9.4 T FT-ICR. The absorption spectra were recorded on a Cary 5000 UV/Vis spectrometer and were baseline and solvent corrected. The fluorescence spectra were recorded on a Varian Cary Eclipse Fluorescence spectrophotometer and emission quantum yields (Φ) were measured on a JASCO spectrofluorometer FP-8500 equipped with an ILF-835j100 mm integrating sphere. Cyclic voltammetry spectra were recorded on a EG&G Princeton Applied Research potentiostat model 263 A using a three-electrode single-component cell under inert atmosphere. A platinum disk was used as working electrode, platinum wire as a counter electrode and a saturated calomel electrode as a reference electrode. As internal reference, ferrocene was used in all cases. Measurements were carried out in a 0.1 M tetrabutylammonium hexafluorophosphate solution in anhydrous dichloromethane under exclusion of oxygen. TGA measurements were performed on a Mettler Toledo TGA 2 device. DSC was performed using a TA Instruments Discovery DSC 250 calorimeter (3b) or a Mettler Toledo DSC821 (2 and 3b) device. X-ray analyses were performed by Priv. Doz. Dr. Joachim Ballmann in the X-ray laboratory of the Department of Inorganic Chemistry at the University of Heidelberg with an Agilent Supernova E diffractometer. The obtained structures were solved and refined by Priv. Doz. Dr. Joachim Ballmann Unless otherwise stated, all preparative work was performed in an inert gas atmosphere in standard Schlenk glassware, which was flame-dried. Octachlorotetraazaperylene 1 was synthesized according to our previously reported procedure.[2,3]

2. Synthesis and Characterization of Compound 1

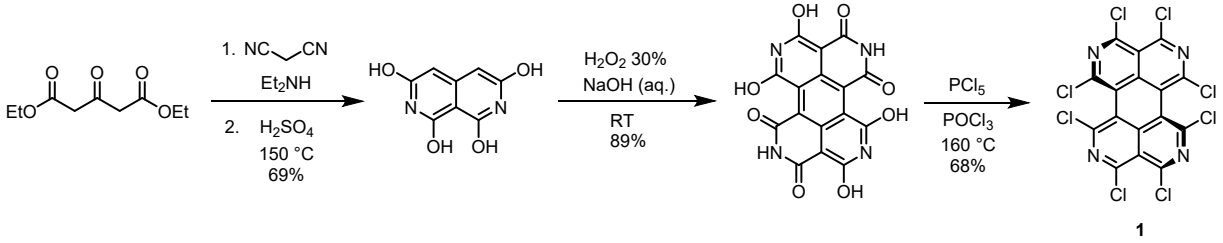

Scheme S1. Synthesis of tetraazaperylene **1**.

2,7-Naphthyridine-1,3,6,8-tetrol. According to a literature procedure,[2] in a round bottom flask diethyl-1,3-acetonedicarboxylate 8 (36 ml, 40 g, 198 mmol, 1.00 equiv.) was dissolved in ethanol (350 ml). After addition of malononitrile (15.7 g, 238 mmol, 1.20 equiv.) and diethyl amine (2.70 ml, 1.88 g, 25.7 mmol, 0.13 equiv.) the reaction mixture was stirred at room temperature for 2 days. The solvent was evaporated under reduced pressure to give a brown oil. After slow addition of 70% sulfuric acid (350 ml) to the residue, the mixture was stirred at 140°C for 20 min. The solution was allowed to reach room temperature, poured into water (400 ml) and the precipitate was filtered. Washing with water (500 ml) followed by drying in vacuo at 70°C gave the title 2,7-naphthyridine-1,3,6,8-tetrol (26.4 g, 136 mmol, 69%) as a beige solid. The NMR spectra are consistent with a mixture of lactam and lactim tautomers: ^{1}H-NMR (DMSO-d_6, 600.18 MHz, 295 K δ [ppm] = 11.38 (s, 2H), 5.77 (s, 2H), 5.51 (s, 2H). ^{13}C-NMR (DMSO-d_6, 150.92 MHz, 295 K) δ [ppm] = 169.6, 169.3, 165.8, 163.6, 162.5, 148.7, 104.7, 88.9, 35.7.

4,10-Dihydroxy-5,11-dihydro-2,5,8,11-tetraazaperylene-1,3,6,7,9,12-hexaone. According to a literature procedure,[3] in a round bottom flask 2,7-naphthyridine-1,3,6,8-tetrol (10.0 g, 51.5 mmol, 1.00 equiv.) was suspended in 0.25 M NaOH (210 ml). Addition of H_2O_2 (6.4 ml, 7.1 g, 206 mmol, 4.00 equiv.) was carried out over a period of 3 h during which the color of the suspension changed from yellow to dark blue. The mixture was stirred for 20 h at room temperature and the resulting precipitate was filtered and washed with water (1 l). Drying under reduced pressure at 70°C gave 4,10-dihydroxy-5,11-dihydro-2,5,8,11-tetraazaperylene-1,3,6,7,9,12-hexaone (9.82 g, 23.0 mmol, 89%) as a dark blue solid. ^{13}C-NMR (D_2SO_4, 150.92 MHz, 295 K) δ [ppm] = 167.3, 162.3, 136.7, 124.7, 88.3.

1,3,4,6,7,9,10,12-Octachloro-2,5,8,11-tetraazaperylene (1). According to a literature procedure,[3] in a pressure flask 4,10-Dihydroxy-5,11-dihydro-2,5,8,11-tetraazaperylene-1,3,6,7,9,12-hexaone (10.0 g, 26.2 mmol, 1.00 equiv.) and PCl_5 (100 g, 481 mmol, 18.4 equiv.) were suspended in $POCl_3$ (100 ml, 164 g, 1.07 mol, 41.0 equiv.) and stirred at 160°C for 2 days. The reaction mixture was poured on ice and the precipitate was filtered. Washing with water, MeOH and pentane followed by drying in vacuo gave compound **1** (9.44 g, 17.8 mmol, 68%) as an orange solid. ^{13}C-NMR (nitrobenzene-d_5, 150.92 MHz, 295 K) δ [ppm] = 148.1, 146.3, 144.4, 116.9, 116.7.

2,7-Naphthyridine-1,3,6,8-tetrol

^{1}H-NMR (DMSO-d_6, 600.18 MHz, 295 K):

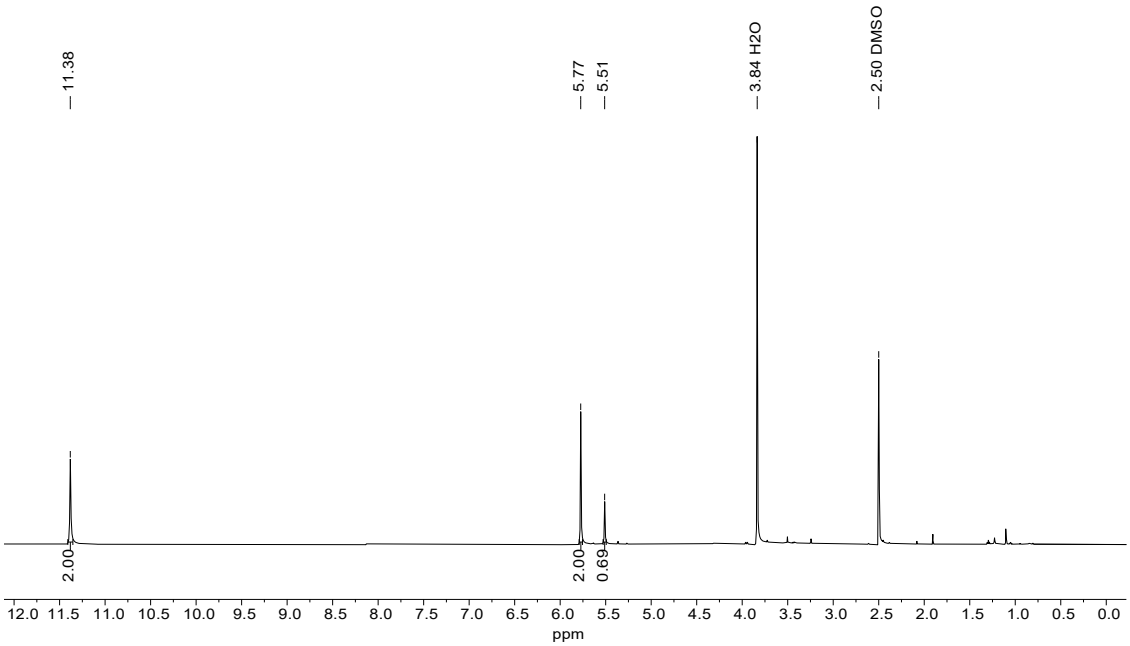

^{13}C-NMR (DMSO-d_6, 150.92 MHz, 295 K):

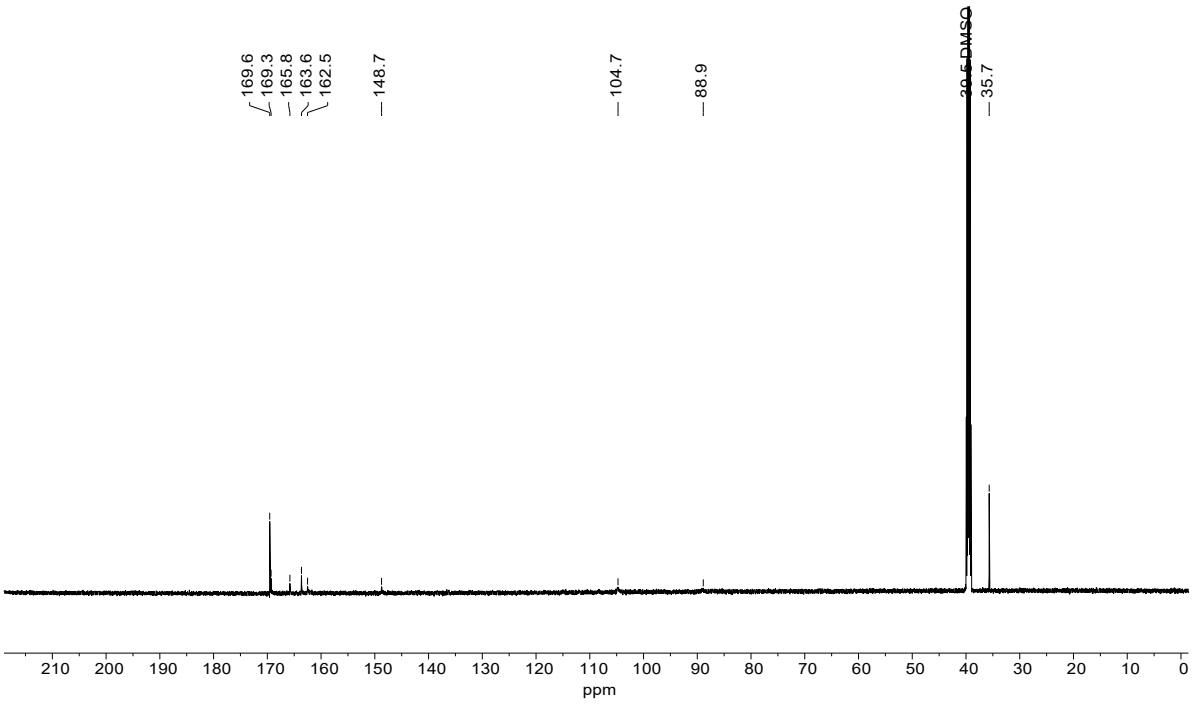

4,10-Dihydroxy-5,11-dihydro-2,5,8,11-tetraazaperylene-1,3,6,7,9,12-hexaone

^{13}C-NMR (D_2SO_4, 150.92 MHz, 295 K):

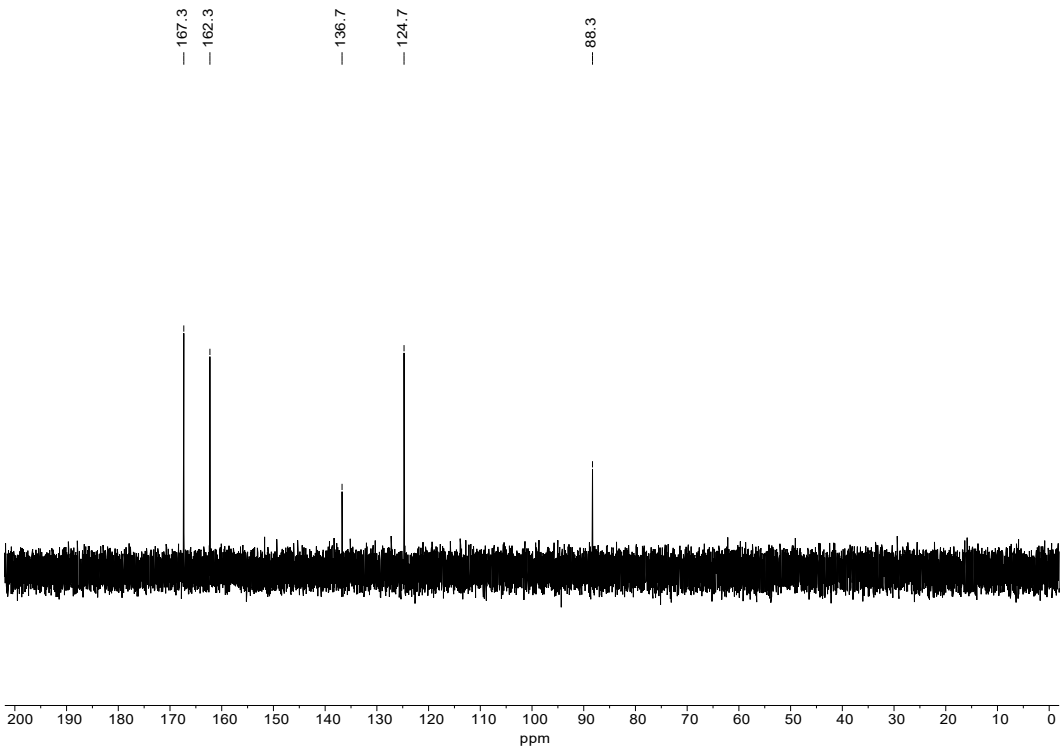

1,3,4,6,7,9,10,12-Octachloro-2,5,8,11-tetraazaperylene (1)

^{13}C-NMR (nitrobenzene-d_5, 150.92 MHz, 295 K):

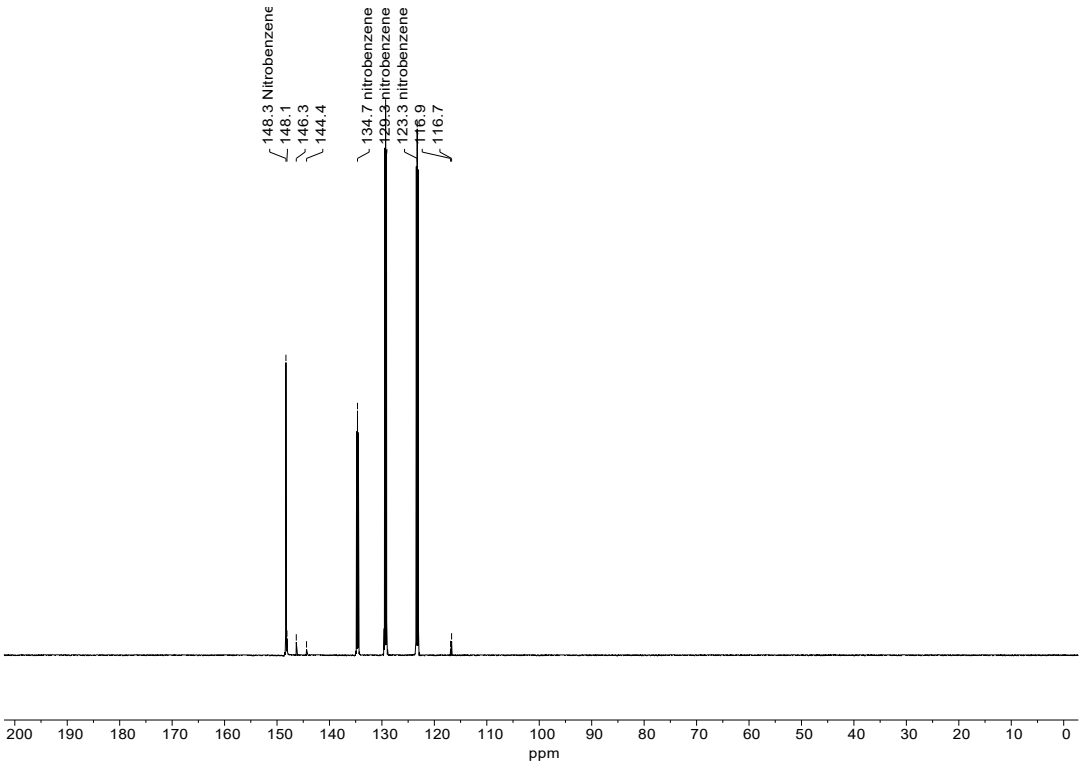

3. Characterization of the Compounds

^{1}H and ^{13}C spectra

Compound **2a**

^{1}H NMR (600.13 MHz, $CDCl_3$ 295 K):

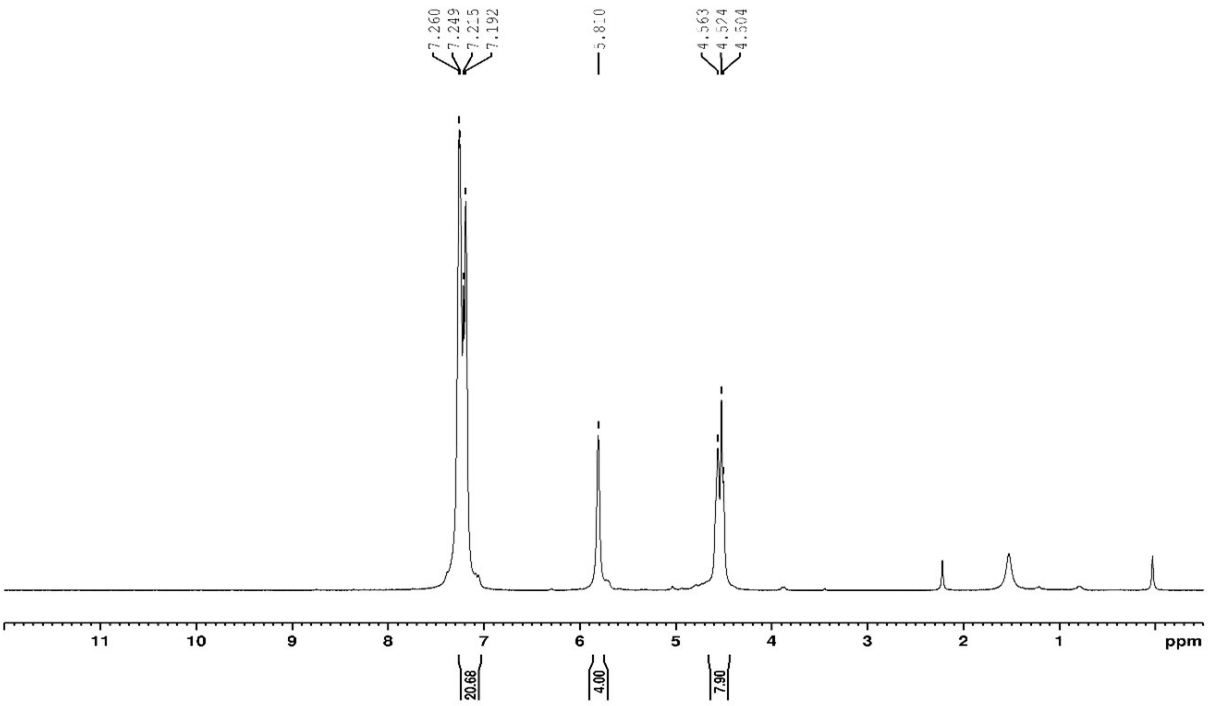

^{13}C NMR (150.90 MHz, $CDCl_3$, 295 K):

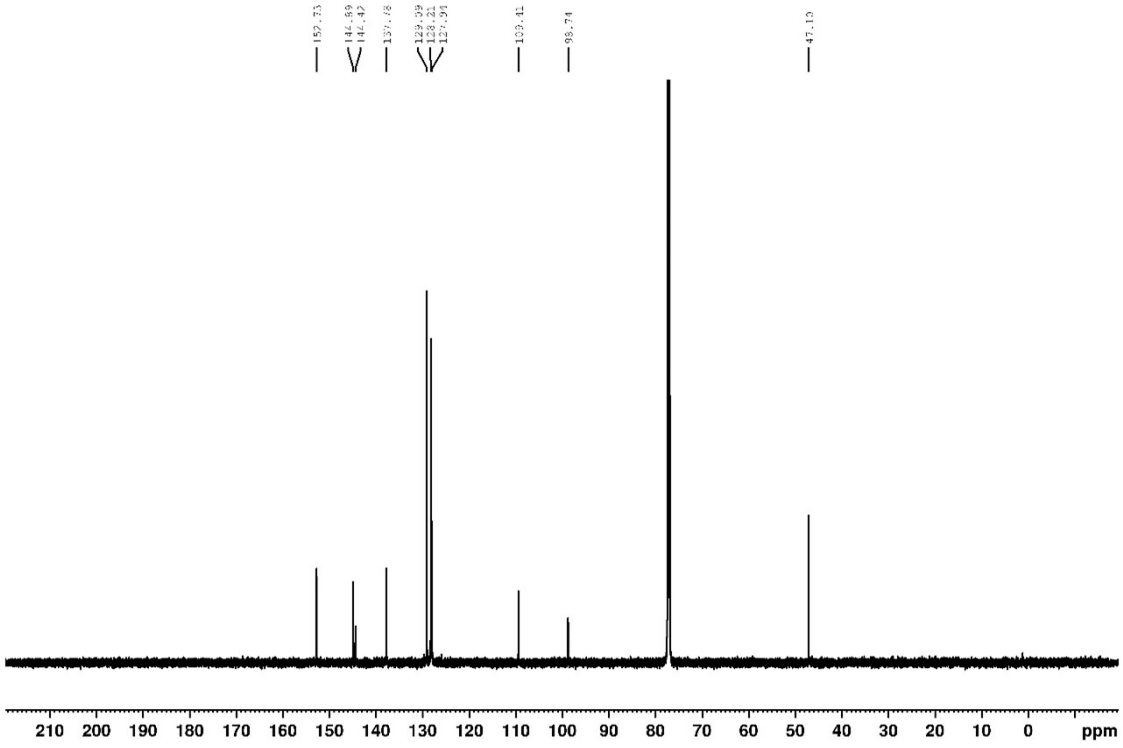
152.73
144.89
142.42
137.48
129.09
128.21
127.93
109.41
98.74
47.13
210 200 190 180 170 160 150 140 130 120 110 100 90 80 70 60 50 40 30 20 10 0 ppm

Compound **2b**

^{1}H NMR (600.13 MHz, $CDCl_3$ 295 K):

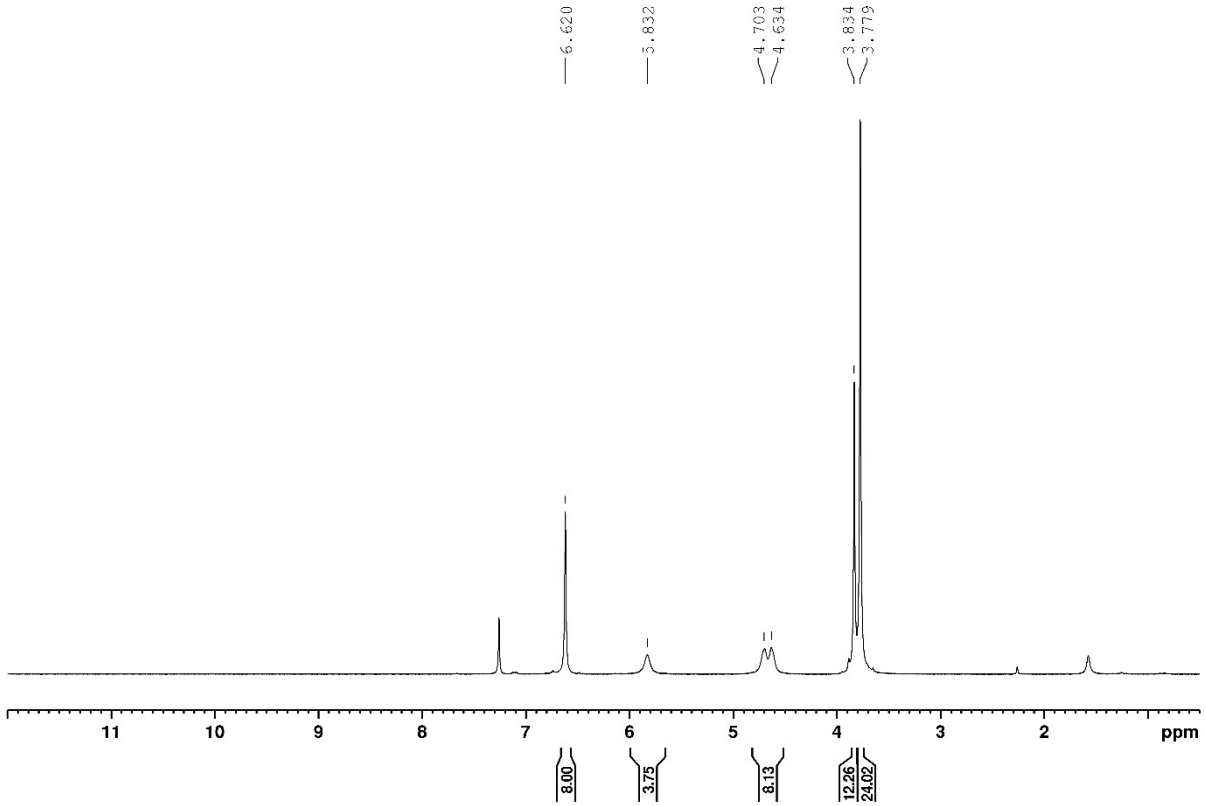

^{13}C NMR (150.90 MHz, $CDCl_3$, 295 K):

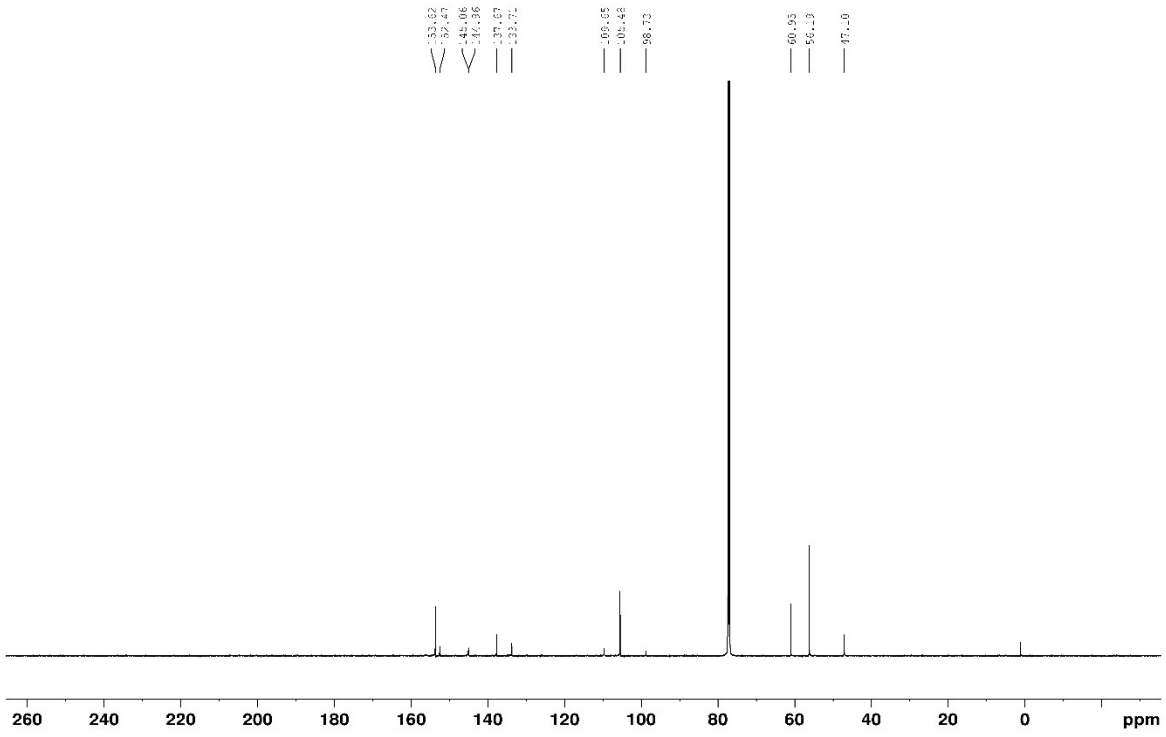
153.62
152.47
145.06
142.96
137.67
133.72
109.65
106.48
98.73
60.93
56.19
47.10
260
240
220
200
180
160
140
120
100
80
60
40
20
0
ppm

Compound **3a**

^{1}H NMR (600.13 MHz, $CDCl_3$ 295 K):

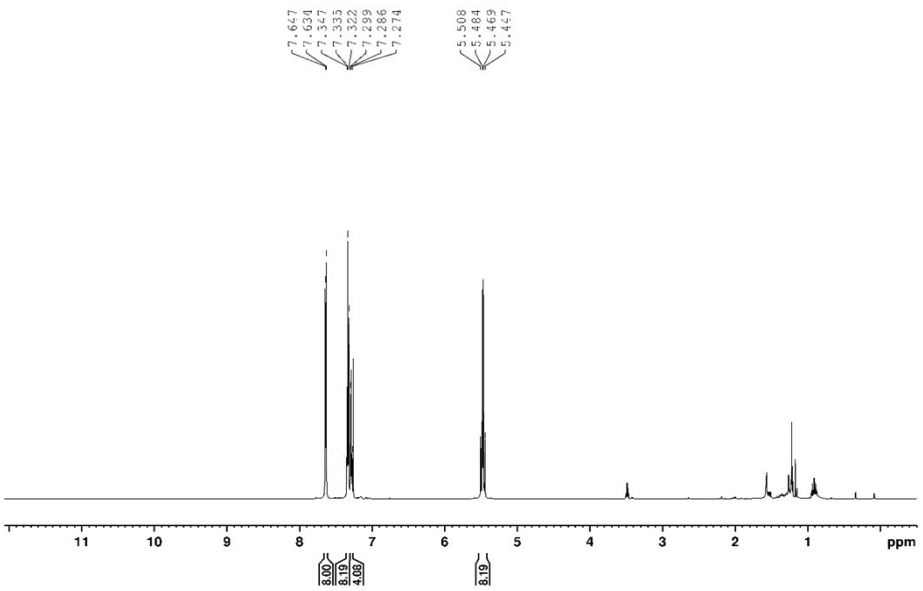

^{13}C NMR (150.90 MHz, $CDCl_3$, 295 K):

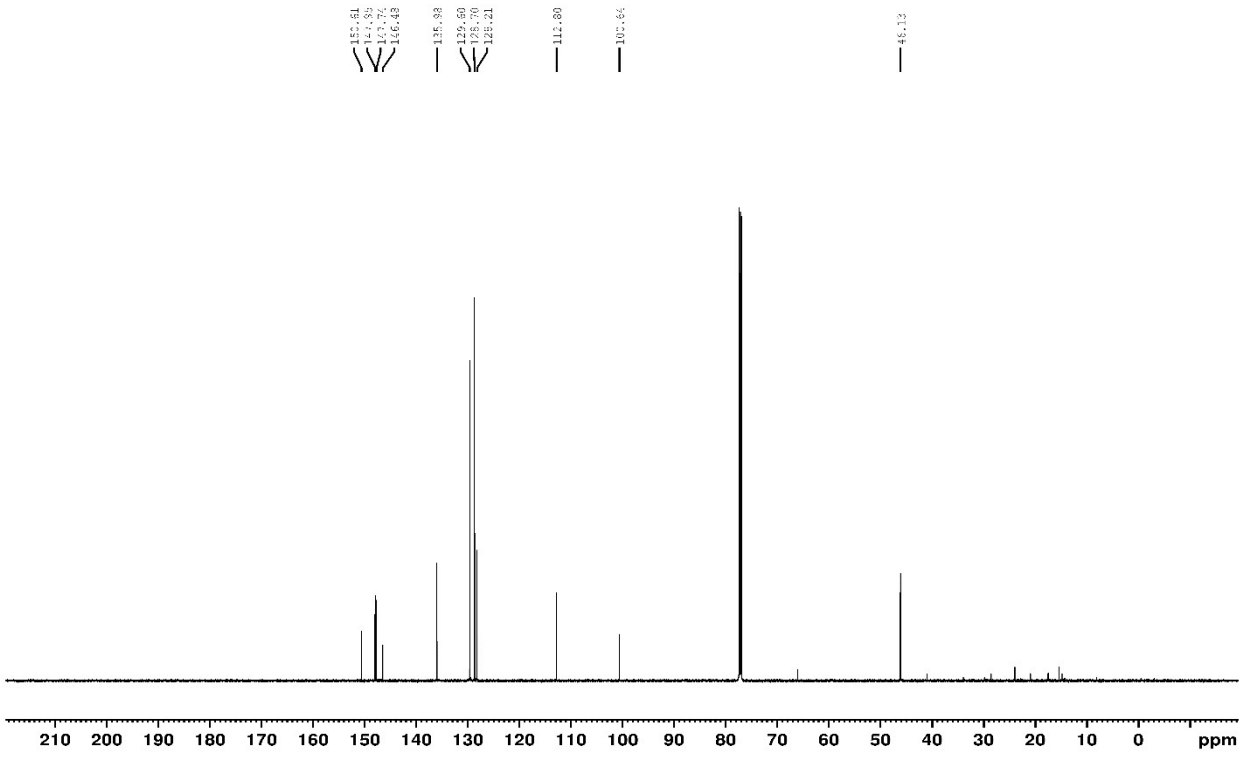

Compound **3b**

^{1}H NMR (600.13 MHz, $CDCl_3$ 295 K):

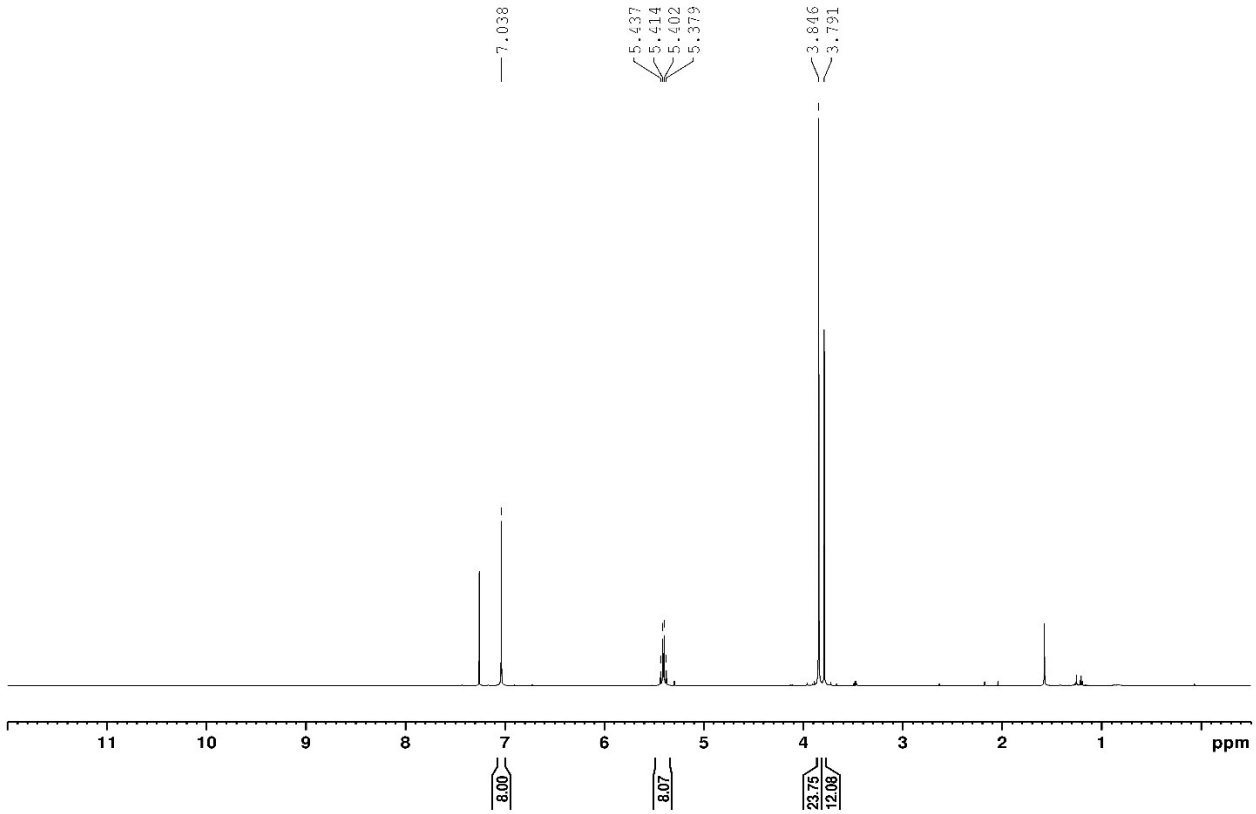

^{13}C NMR (150.90 MHz, $CDCl_3$, 295 K):

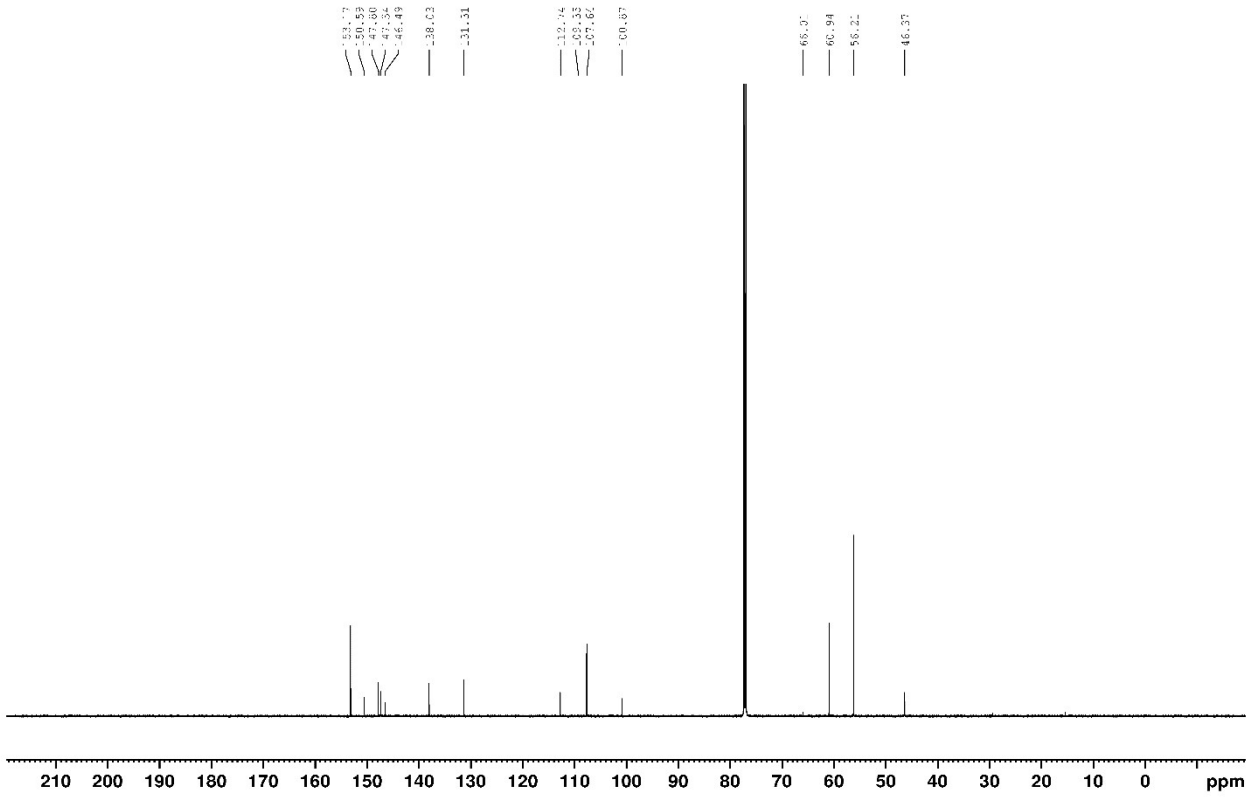

IR Spectra

Compound **2a**

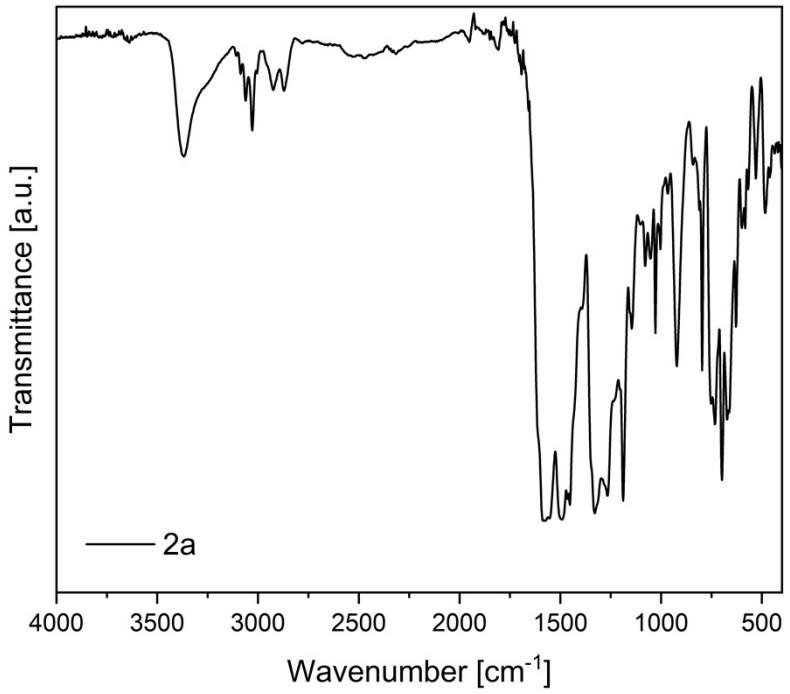

Compound **2b**

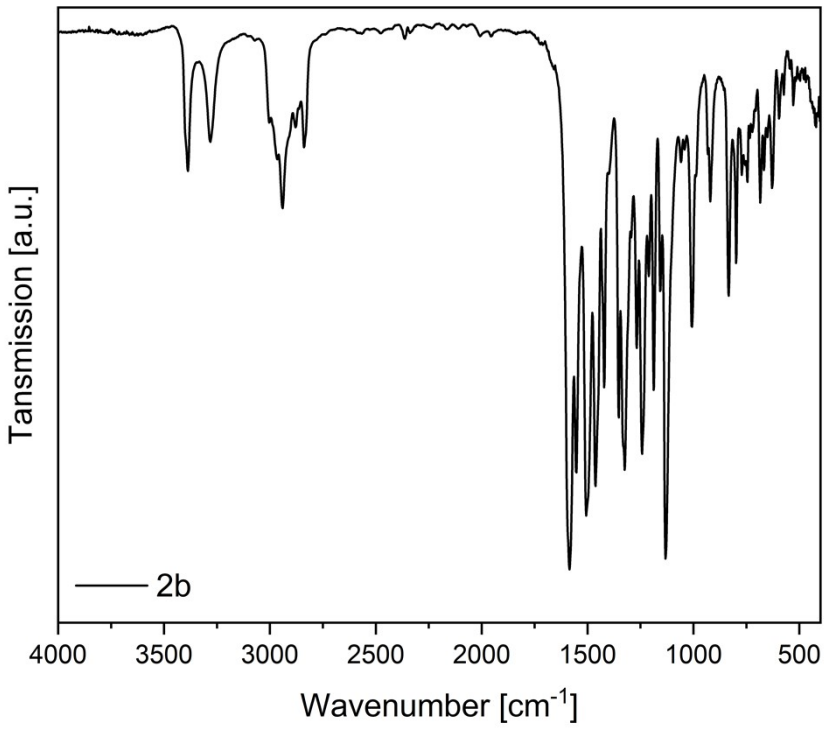

Compound **3a**

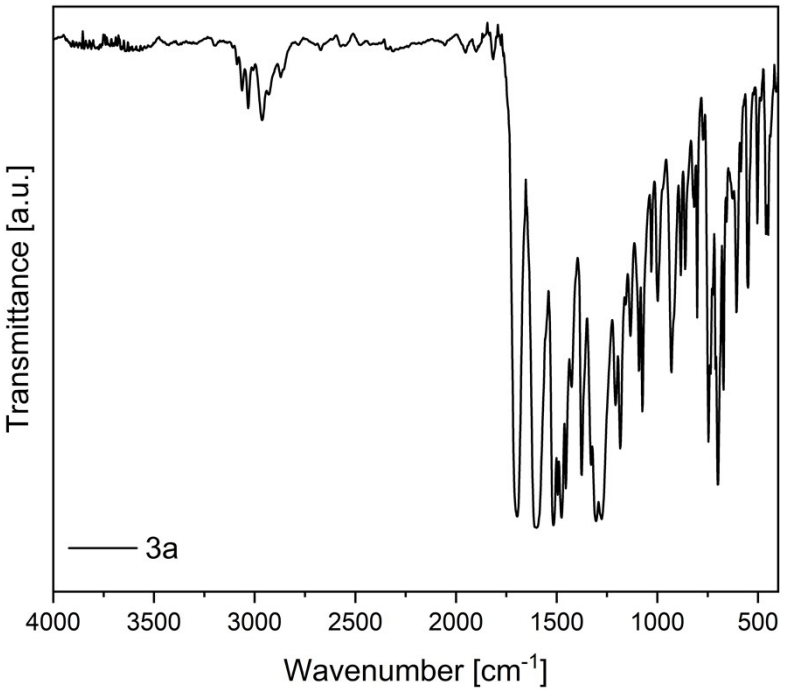

Compound **3b**:

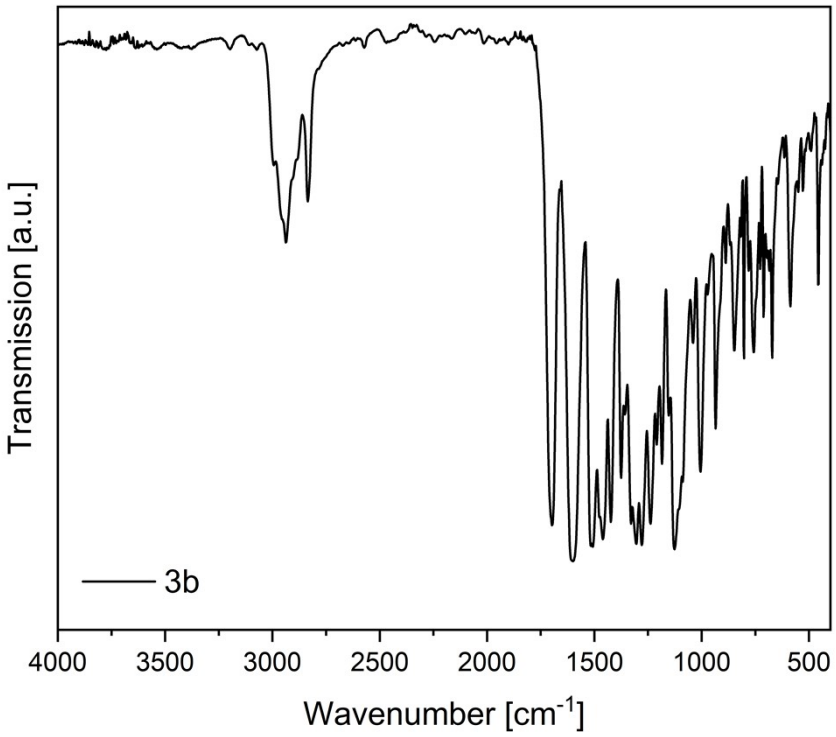

Computational Data

Except the excited state dynamics (ESD) all DFT calculations were performed using the Gaussian 16 program suit (G16RevC.01).[4] The B3LYP[5] functional was used to optimize the geometries on the valence double/triple-ζ basis sets Def2-SVP[6], Def2-TZVP[6] and Def2-TZVPP[6] including one or two sets of polarization functions. The resulting ground state structures were confirmed as energy minima through frequency calculations showing no negative eigenvalue in the Hessian matrix. Grimme's dispersion correction D3[7] with Becke-Johnson damping[8] were considered in all calculations and inspected with respect to the influence of solvent effects (CPCM[9] for dcm as implemented in Gaussian).

TD-DFT calculations for molecular properties on the excited state were performed at the triple-ζ level of theory (Def2-TZVPP) with B3LYP using 10 roots for singlet excitations.

Dynamic properties of the absorption and emission spectra of 3a were simulated with the Excited State Dynamic (ESD) module as implemented in ORCA 4.2.1.[10] using B3LYP and Def2-SVP as well as the RIJCOSX approximation[11]. Additionally, the auxiliary basis set def2/J[12] was employed to decrease computation time. The line shapes of the ESD spectra were adjusted with the flags "LINES VOIGT", "LINEW" and "INLINEW".

Excited State Simulations

TD-DFT Spectra

TD-DFT calculations were performed considering only singlet excited states at the B3LYPGD3(BJ)/Def2-TZVPP (for UV/Vis absorption spectra) level of theory. The optimized ground state structures (same level of theory) were used for all TD-DFT calculations. UV/Vis spectra were depicted using ChemCraft (v1.8).[13] with a band width on ½ height of 13 and the same programme was used for visualizing molecular structures.

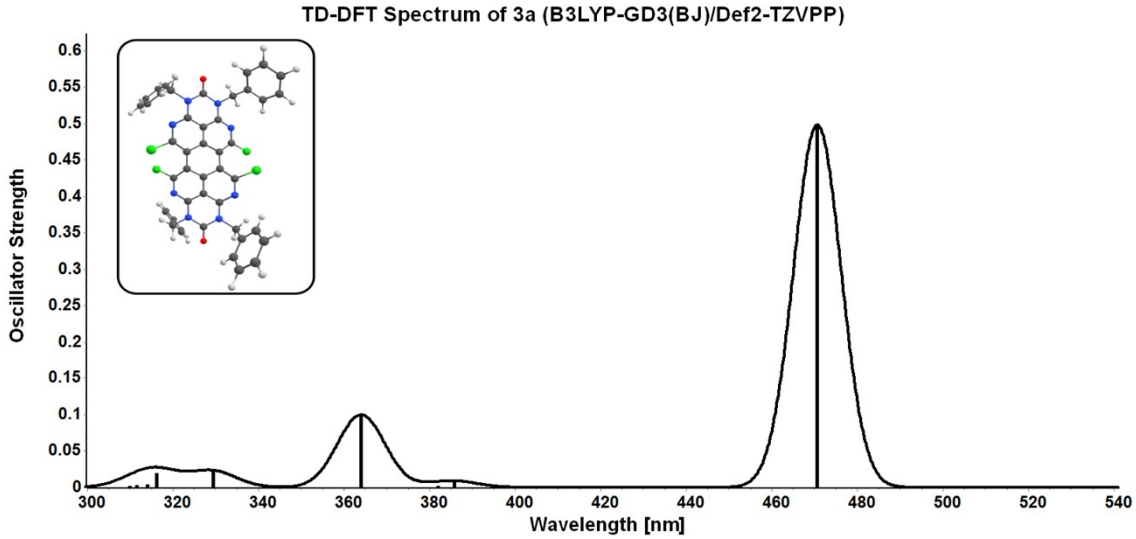

Figure S1. Visualization of the TD-DFT UV/Vis spectrum of **3a** in the gas phase.

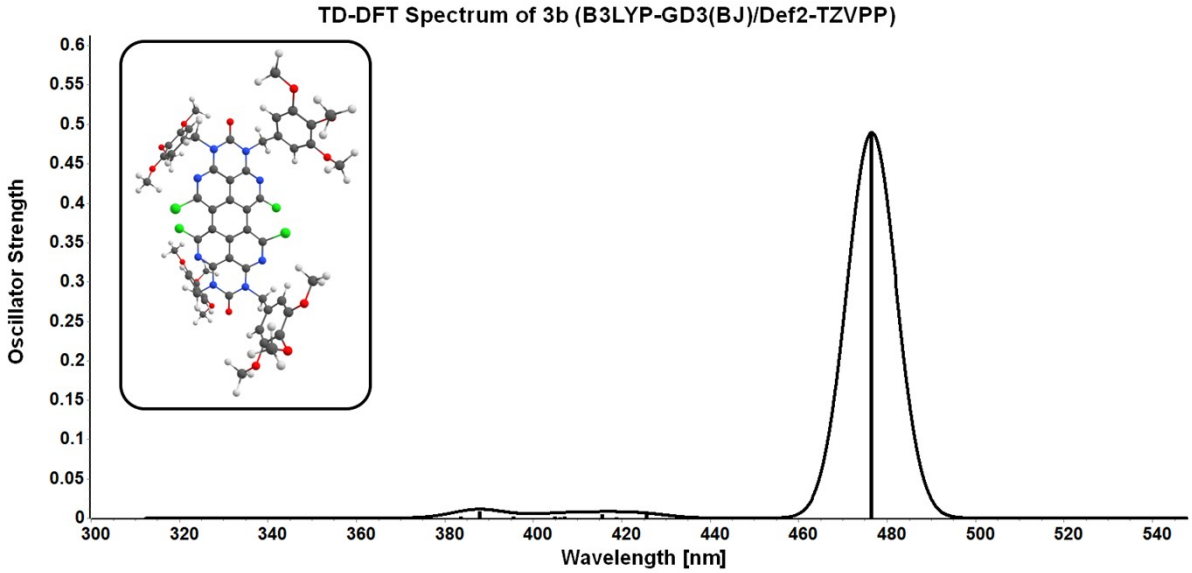

Figure S2. Visualization of the TD-DFT UV/Vis spectrum of **3b** in the gas phase.

Table S1. The first 10 excited states (singlets) of **3a** (B3LYP-GD3(BJ)/Def2-TZVPP level of theory, gas phase):

Excited State	Wavelength [nm]	Oscillator Strength
1	470.62	0.4985
2	385.86	0.0077
3	381.97	0.0017
4	364.00	0.0997
5	348.55	0.0000
6	329.38	0.0223
7	316.23	0.0197
8	314.01	0.0038
9	311.64	0.0027
10	309.97	0.0024

Table S2. The first 10 excited states (singlets) of **3b** (B3LYP-GD3(BJ)/Def2-TZVPP level of theory, gas phase):

Excited State	Wavelength [nm]	Oscillator Strength
1	476.49	0.4898
2	425.57	0.0048
3	418.85	0.0014
4	415.59	0.0048
5	407.12	0.0021
6	406.05	0.0012
7	404.89	0.0021
8	395.53	0.0022
9	387.87	0.0087
10	383.63	0.0022

Excited State Dynamics (ESD)

The additional features of the experimental spectrum which could not be simulated by TD-DFT modelling can be calculated by consideration of dynamic effects such as vibronic coupling. This was done exemplarily for compound **3a** through ESD (excited state dynamics) calculations. To reduce the computational cost, they were performed at the B3LYP-GD3(BJ)/Def2-SVP level of theory. Furthermore, *N*-hexyl substituents were replaced by *N*-methyl groups. The hessians of the frist five excited states were approximated via the vertical gradient model. For each coupling of the S_0 and $S_{1\text{-}5}$ state the resulting spectra were then predicted using the first five excitations. The resulting spectra are shown in figure SI 3. Based on the modelling, the spectrum can be well described by a mixture of the vibronic coupling between S_0 and S_1, as well as S_0 and S_2. Coupling with higher excited sates show similar spectral features.

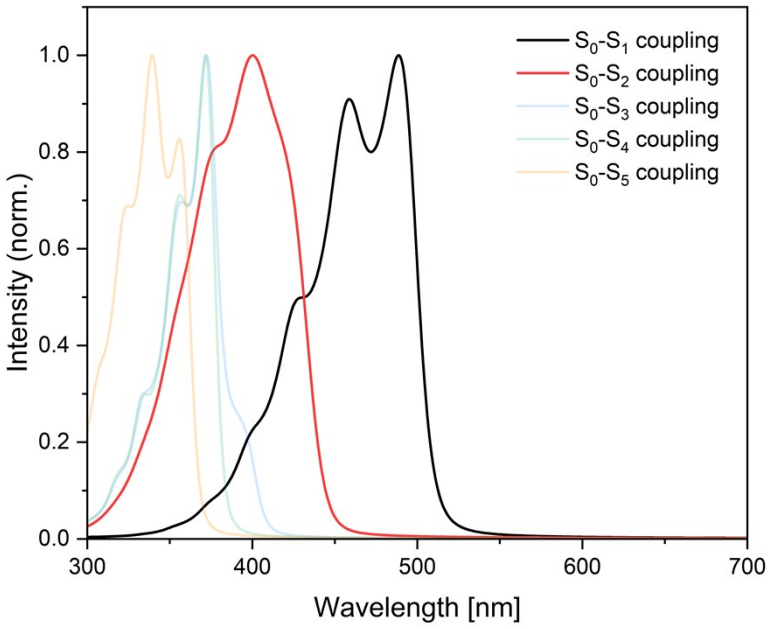

Figure S3. UV/Vis Spectra for **3a** computed with the ESD module (B3LYP-GD3(BJ)/Def2-SVP) implemented in Orca using the excited state hessians for S_1 to S_5. The first five singlet excitations were considered for each simulation.

Compositions of the photoresists containing OAPPDOs

Table S3: Exact composition in wt% of the photoresists containing OAPPDOs studied in this work.

OAPPDO	OAPPDO [wt%]	DCB [wt%]	PETA [wt%]	BAPO [wt%]
2a	2.3	11.9	84.2	1.7
2b	2.1	11.7	84.5	1.7
3b	2.2	12.0	84.1	1.7

OAPPDO: octaazaperopyrenedioxides; DCB: 1,2-dichlorobenzene; PETA: pentaeritritol triacrylate; BAPO: diphenyl(2,4,6-trimethylbenzoyl)phosphine oxide

Determination of the embedding of tetraazaperylene dyes in microstructures by confocal microscopy

The comparison of the fluorescence intensity was carried out using fixed magnification, excitation strength and receiver gain.

z-Projection images were computed from the measured image sets using a maximum intensity per pixel function. The function being non-sensitive to the number of slides, the complete image sets were considered. From the *z*-projection images, an average intensity value was measured over one microprinted structure (squared piling of rods [40 × 40 µm^2]) and over a fixed area of 327 × 327 px^2.

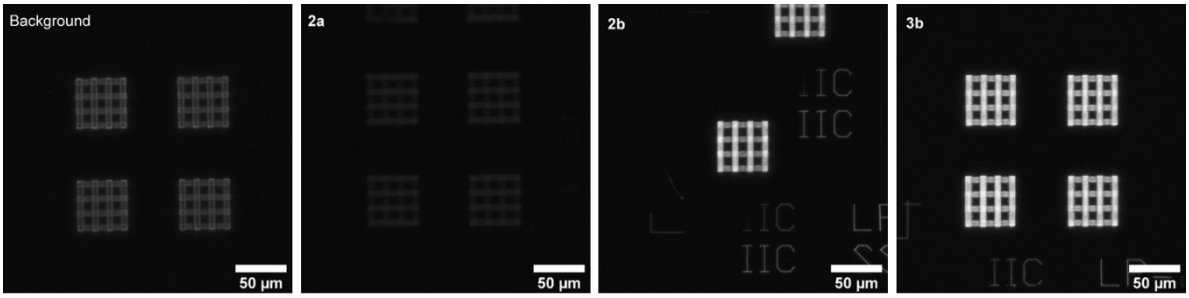

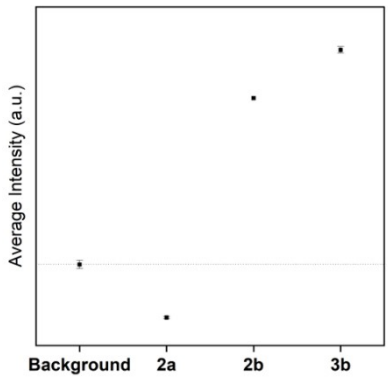

Photoresist	Background	2a	2b	3b
Measurement 1	50.832	23.610	126.895	149.297
Measurement 2	48.235	23.548	—	150.051
Measurement 3	46.147	23.047	—	147.850
Measurement 4	47.901	22.63	—	151.460
Mean value	48.27875	23.209	126.895	149.664
Standard deviation	1.933	0.461	0	1.506

Figure S4. Top: *z*-projection of the image sets for, from left to right, a PETA/BAPO resist, a photoresist containing **2a**, a photoresist containing **2b** and a photoresist containing **3b**. Bottom left: Plot of the mean value of the average fluorescence intensity for the different structures, the dotted line represents the value for the background measurement, for easier comparison. Bottom left: corresponding intensity measurement data.

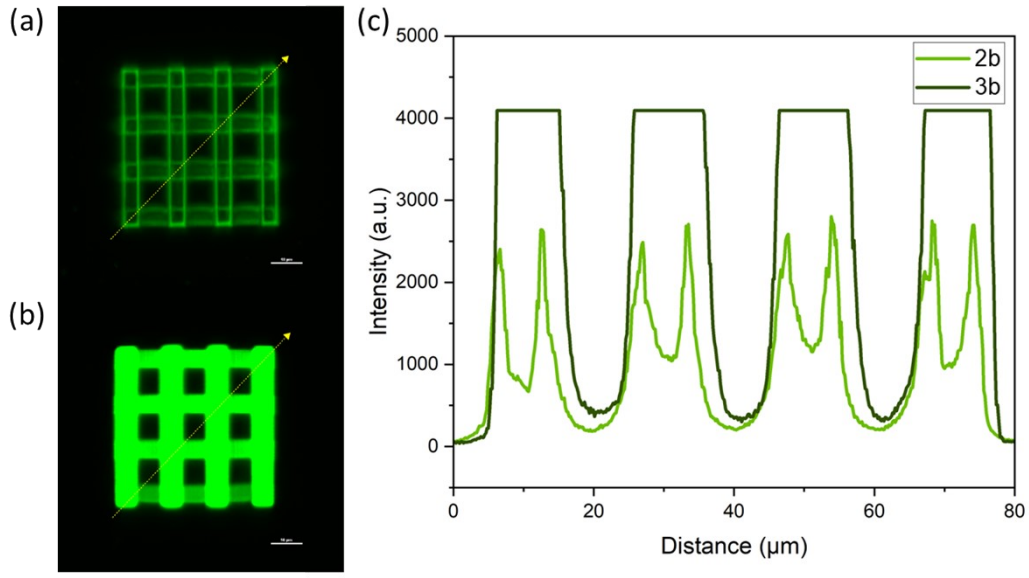

Figure S5. Fluorescence images (a)(b) and their intensity profile (c) of the woodpile structure embedded with **2b** and **3b** while using the excitation condition. (λ_{ex} = 489 nm, laser power: 1.0 %, gain: 10)

Optimized Coordinates at B3LYP-GD3(BJ)/Def2-TZVPP level of theory

xyz-coordinates for **3a**:

atom	x	y	z
C	1.549873	1.691877	1.660213
C	1.430602	0.000007	0.000001
C	3.519326	-0.874575	-0.854823
C	1.549869	-1.691864	-1.660211
N	2.882719	1.647042	1.710008
N	2.882714	-1.647027	-1.710012
C	3.519328	0.874589	0.854818
C	2.831444	0.000007	-0.000001
C	-1.355686	0.000006	0.000006
C	-1.474321	2.305846	0.550091
N	-2.807374	2.324385	0.486293
C	-3.444458	1.190497	0.28321
C	-2.756565	0.000006	0.000008
C	-3.444458	-1.190486	-0.283193
C	-1.474321	-2.305835	-0.550077
N	-2.807375	-2.324374	-0.486276
Cl	0.840888	-2.582596	-2.973098
Cl	-0.765034	3.89213	0.596054
Cl	0.840897	2.58261	2.973102
Cl	-0.765034	-3.892118	-0.596042
C	5.652708	1.820246	1.655445
C	5.652704	-1.820227	-1.655461
C	-5.585358	2.399639	0.529875
C	-5.585354	-2.399632	-0.529855

C	5.792182	-3.164859	-0.986758
C	5.792176	3.164878	0.986741
C	-5.821726	3.181021	-0.739537
C	-5.821665	-3.181049	0.739546
C	6.775049	3.368529	0.017755
C	6.889562	4.598434	-0.616889
H	7.445837	2.558676	-0.235272
C	6.025384	5.637172	-0.287801
C	5.047664	5.441411	0.679965
C	4.930665	4.210092	1.313722
H	4.162841	4.050995	2.05791
C	4.930668	-4.210074	-1.313728
C	6.775068	-3.36851	-0.017785
C	6.88959	-4.598415	0.616857
H	7.445858	-2.558656	0.235234
C	6.025408	-5.637153	0.287781
C	5.047676	-5.441393	-0.679973
H	4.162834	-4.050977	-2.057907
C	-4.962847	-4.217934	1.10129
C	-5.174503	-4.927621	2.276894
H	-4.123193	-4.456847	0.464313
C	-6.245238	-4.606732	3.10271
C	-7.107126	-3.575814	2.745845
C	-6.898162	-2.867097	1.569625
H	-7.565175	-2.063499	1.290426
C	-6.898236	2.867016	-1.569579
C	-7.107256	3.575699	-2.745809
H	-7.565216	2.063403	-1.290342
C	-6.245411	4.606636	-3.102722
C	-5.174664	4.927579	-2.276943
C	-4.962952	4.217926	-1.101329
H	-4.123288	4.456881	-0.46438
N	-4.822087	1.154925	0.291639
N	-4.822087	-1.154916	-0.291616
N	4.896876	0.86408	0.818806
N	4.896874	-0.864064	-0.818816
C	5.624303	0.000007	-0.000005
C	-5.548164	0.000004	0.000015

xyz-coordinates for **3b**:

atom	x	y	z
C	-1.667817	1.136616	-2.048678
C	-0.846582	0.779112	-0.975006
C	-1.481309	-0.036831	0.005912
C	-3.532196	-0.768255	1.063012
C	-0.760068	-0.784603	0.983355
C	-1.533905	-1.224584	2.059273
N	-2.994813	1.005662	-2.083126

N	-2.866375	-1.237964	2.098104
C	-3.601811	0.454958	-1.052693
C	-2.880028	-0.115113	0.006763
C	0.570409	1.057295	-0.768619
C	0.673815	-0.925507	0.763103
C	1.302427	0.099125	-0.006476
C	1.316345	2.171284	-1.160377
N	2.645311	2.267284	-1.117188
C	3.336242	1.26349	-0.616846
C	2.701751	0.165409	-0.013478
C	3.443852	-0.868795	0.579724
C	1.525648	-1.963371	1.143529
N	2.856988	-1.935181	1.084883
Cl	-0.796354	-1.703598	3.560717
Cl	0.532447	3.655404	-1.621501
Cl	-0.989059	1.680614	-3.552056
Cl	0.890939	-3.519541	1.609077
C	-5.771312	1.057423	-2.059325
C	-5.608877	-1.675769	2.036068
C	5.419587	2.465379	-1.188748
C	5.638777	-1.86833	1.120983
C	-5.5693	-3.142734	1.690647
C	-5.992357	2.508579	-1.718939
C	5.596203	3.567488	-0.174266
C	5.899697	-2.948102	0.10032
C	-6.97141	2.854753	-0.784941
C	-7.155237	4.186114	-0.438739
H	-7.582719	2.079245	-0.352471
C	-6.350339	5.193674	-1.008607
C	-5.372599	4.830985	-1.939435
C	-5.204108	3.489725	-2.291142
H	-4.430917	3.240693	-3.002449
C	-4.549005	-3.941182	2.194228
C	-6.519452	-3.670147	0.821426
C	-6.445916	-5.013109	0.452718
H	-7.294885	-3.028171	0.435159
C	-5.423661	-5.828408	0.95551
C	-4.466661	-5.281112	1.817458
H	-3.816889	-3.505058	2.852401
C	5.033622	-4.038277	0.012149
C	5.243847	-5.022964	-0.94706
H	4.192402	-4.091996	0.682646
C	6.334328	-4.923465	-1.827082
C	7.198526	-3.833219	-1.723047
C	6.983624	-2.849326	-0.761663
H	7.65944	-2.008158	-0.714265
C	6.692687	3.54569	0.682379
C	6.838601	4.546677	1.641978
H	7.409379	2.745325	0.598885

C	5.893169	5.575114	1.738518
C	4.789538	5.57898	0.877906
C	4.646504	4.579079	-0.083195
H	3.796848	4.562571	-0.744562
O	8.238445	-3.679848	-2.601062
O	6.570364	-5.899448	-2.756827
O	4.443099	-6.106896	-1.116622
O	-7.317346	-5.620659	-0.392681
O	-5.385176	-7.157107	0.642204
O	-3.488529	-6.126301	2.231049
O	-4.581028	5.721247	-2.599092
O	-6.590343	6.516885	-0.754022
O	-8.118325	4.618563	0.419628
O	6.069596	6.591957	2.63345
O	7.865324	4.60798	2.528812
O	3.905168	6.593745	1.055359
C	9.306368	-4.619439	-2.460011
H	10.04304	-4.357781	-3.215671
H	8.957319	-5.638879	-2.619823
H	9.757777	-4.533543	-1.46803
C	5.763057	-5.805795	-3.932116
H	6.062421	-6.628358	-4.577059
H	5.941001	-4.856469	-4.442139
H	4.705103	-5.902588	-3.684162
C	3.311168	-6.234972	-0.270062
H	3.607429	-6.321462	0.777909
H	2.809113	-7.147016	-0.580283
H	2.63207	-5.386565	-0.378918
C	-4.653801	-7.464118	-0.543012
H	-4.704689	-8.543197	-0.667283
H	-3.609866	-7.157669	-0.442998
H	-5.101025	-6.975761	-1.411745
C	-2.466886	-5.602061	3.064661
H	-1.784422	-6.426243	3.252404
H	-2.871015	-5.243622	4.014144
H	-1.92967	-4.786462	2.575025
C	-8.38244	-4.848297	-0.920087
H	-8.950615	-5.520082	-1.557323
H	-8.012096	-4.008836	-1.513781
H	-9.028804	-4.467748	-0.125633
C	-8.99688	3.655497	0.978237
H	-9.684008	4.210422	1.610779
H	-8.455096	2.923448	1.581728
H	-9.558192	3.13375	0.200007
C	-6.354685	6.968402	0.580671
H	-6.533705	8.040855	0.572644
H	-5.319281	6.775652	0.874091
H	-7.029442	6.487487	1.285798
C	-4.00308	6.814458	-1.890257

H	-3.146149	7.129839	-2.481578
H	-3.65867	6.497325	-0.903181
H	-4.704111	7.638918	-1.783838
C	8.864076	3.604296	2.460598
H	9.578532	3.841314	3.243985
H	9.370395	3.612451	1.492474
H	8.445364	2.610404	2.636784
C	5.508041	6.349475	3.921428
H	5.720419	7.230371	4.522687
H	5.966102	5.472836	4.38513
H	4.426848	6.20833	3.851414
C	2.768336	6.638372	0.208481
H	2.198627	7.508963	0.521497
H	2.153822	5.741245	0.313367
H	3.05681	6.75104	-0.839308
N	4.712618	1.292715	-0.623499
N	4.816286	-0.766875	0.571782
N	-4.976873	0.372066	-1.016167
N	-4.904791	-0.866821	1.015294
C	-5.666057	-0.29986	-0.007095
C	5.490366	0.301515	-0.024178
H	6.566522	-1.418409	1.455574
H	5.096986	-2.264582	1.973632
H	6.378052	2.102108	-1.542282
H	4.826521	2.806605	-2.03062
H	-5.220638	0.959008	-2.988697
H	-6.710864	0.520813	-2.130046
H	-5.115188	-1.484765	2.983399
H	-6.626441	-1.304751	2.071499
O	6.702257	0.363549	-0.019798
O	-6.878497	-0.386826	-0.016483

Crystal Structure of Compounds 3a

Single crystals of compound **3a** were grown from a concentrated solution of **3a** in chlorobenzene. Full shells of intensity data were collected at low temperature with an Agilent Technologies Supernova-E CCD diffractometer (Cu-K_α radiation, microfocus X-ray tubes, multilayer mirror optics). Detector frames (typically ω-, occasionally φ-scans, scan width 1°) were integrated by profile fitting.[14,15] Data were corrected for air and detector absorption, Lorentz and polarization effects[15] and scaled essentially by application of appropriate spherical harmonic functions.[16,17] Absorption by the crystal was treated numerically (Gaussian grid).[16,18] An illumination correction was performed as part of the absorption correction.[16]

Using Olex2-1.5,[19] the structure was solved with SHELXT[20] (intrinsic phasing) and refined with SHELXL[21] by full-matrix least squares methods based on F^2 against all unique reflections. All non-hydrogen atoms were given anisotropic displacement parameters. Hydrogen atoms were generally input at calculated positions and refined with a riding model.[22] Split atom models were used to refine disordered groups and/or solvent molecules. When found necessary, suitable geometry and adp restraints were applied.[22,23]

Due to severe disorder and fractional occupancy, electron density attributed to four PhCl molecules per asymmetric unit (two PhCl molecules per formula unit) was removed from the structure using Olex2 solvent masks (an Olex2 implementation of the BYPASS procedure).[24] Upon structure solution with SHELXT[20], overall eight PhCl molecules were found in the asymmetric unit, but severe issues were encountered in the later stages of the refinement, presumably due to fractionally occupied positions or due to the presence of minor amounts of benzene or toluene. Hence, negative difference Fourier peaks were found on some of the chlorine atoms, rendering the use of solvent masks inevitable. In this context, it needs to be mentioned that the atom positions of the main residue were not affected by masking some or even all of the PhCl solvents, while the residual densities at the lighter atoms were found to be affected to some extent. The latter effect seemed to be related to the solvent mask and to the unmasked PhCl molecules, which was investigated in detail by masking different pairs of PhCl molecules. Overall four PhCl molecules per asymmetric unit (two PhCl per formula unit) were include in the refinement, while four PhCl molecules had to be masked. Three out of the four refined PhCl solvents were found to be disordered, which was modeled by considering two positions for each of the disordered PhCl solvents. Disorder over more than two positions (or PhCl/benzene/toluene disorder), however, cannot be excluded. In Figure S8, the difference Fourier map is shown together with the final model.

Crystals of this compound were also grown in the absence of chlorinated solvents. These crystals, however, did not diffract well (diffraction limit of approximately 1.2 Å), which is more frequently observed for azaperylene derivatives. Hence, we intentionally co-crystallized chlorobenzene to improve scattering at higher angles, which led to the data set reported herein.

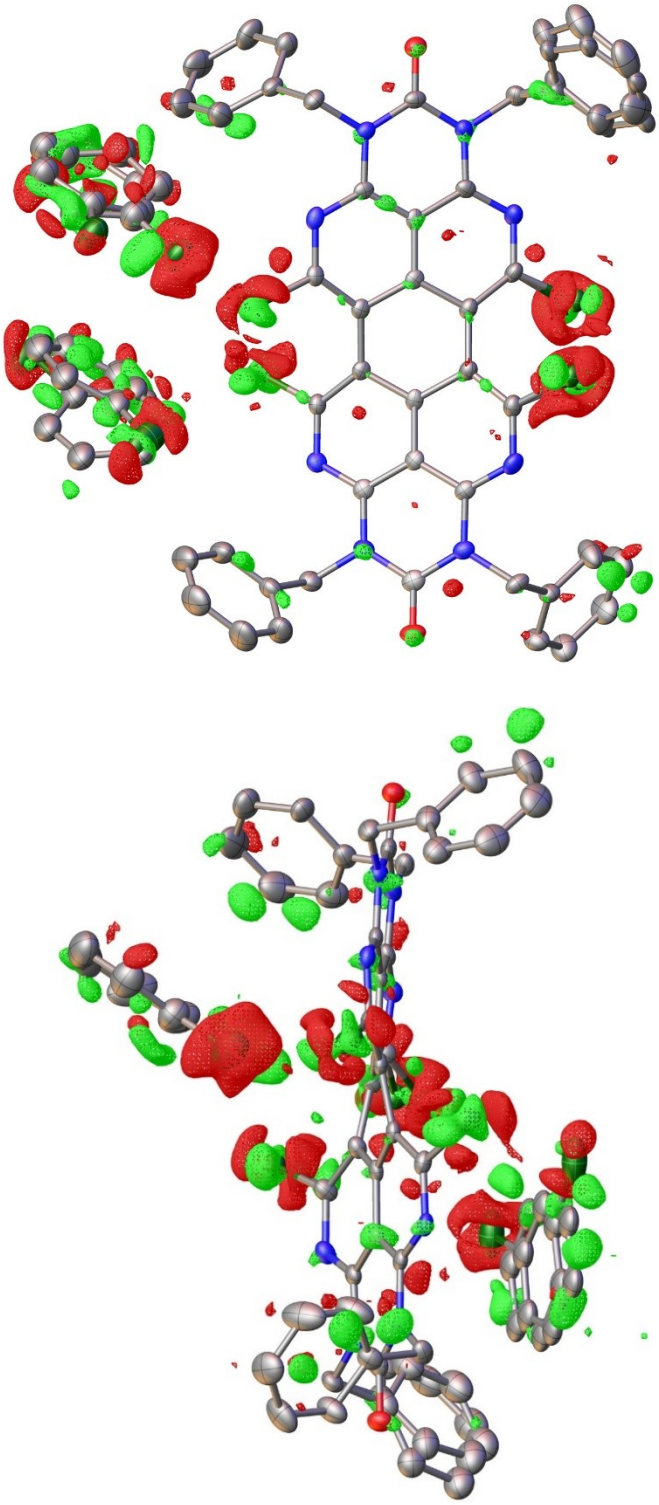

Figure S6. Illustration of the residual electron densities in **3a**. In addition to four masked PhCl solvents, two molecules of **3a** and four (refined) PhCl solvents are present in the asymmetric unit. For clarity, one molecule (with two refined PhCl solvents) is shown in the upper half of the figure, while the other molecule (with two refined PhCl solvents) is shown in the lower half of the figure. To illustrate that only minor residual densities are found at the lighter atoms, an isovalue of 0.29 was chosen for drawing the difference Fourier map. The largest hole and the highest peak correspond to 0.82 and –0.71 electrons, respectively.

CCDC 2255864 contains the supplementary crystallographic data for this paper. These data can be obtained free of charge from the Cambridge Crystallographic Data Centre's and FIZ Karlsruhe's joint Access Service via https://www.ccdc.cam.ac.uk.

Table S4. Details of the crystal structure determinations of compound **3a**.

	3a
Empirical formula	$C_{70}H_{48}Cl_8N_8O_2$
Formula weight	1316.76
Temperature [K]	120(1)
Crystal system	monoclinic
Space group (number)	$P2_1/c$ (14)
a [Å]	28.9316(3)
b [Å]	13.97170(10)
c [Å]	31.8610(4)
α [°]	90
β [°]	108.0840(10)
γ [°]	90
Volume [Å3]	12242.8(2)
Z	8
ρ_{calc} [gcm−3]	1.429
μ [mm−1]	3.805
transmission factors (max, min)	1.000, 0.613
F(000)	5408
Radiation	Cu-K_α (λ = 1.54184 Å)
2θ range [°]	7.0 to 141.9 (0.82 Å)
Index ranges	$-35 \le h \le 35$
	$-17 \le k \le 17$
	$-38 \le l \le 39$
Reflections collected	263094
Independent reflections	23414 (R_{int} = 0.066)
observed [$I \ge 2\sigma(I)$]	17299
Completeness to θ = 67.68°	99.8 %
Data / Restraints / Parameters	23414 / 323 / 1343
Goodness-of-fit on F^2	1.060
Final R indexes [$I \ge 2\sigma(I)$]	R_1 = 0.0711, wR_2 = 0.1982
Final R indexes [all data]	R_1 = 0.0877, wR_2 = 0.2165
Largest peak/hole [eÅ^{-3}]	0.82/−0.71
CCDC number	2255864

Thermogravimetric Analysis and Differential Scanning Calorimetry

Thermogravimetric analysis (TGA) and differential scanning calorimetry (DSC) of compounds **2** and **3** were performed under the heating/cooling conditions described in the caption of the corresponding figure. The samples were measured in an aluminum pan. For DSC measurements the pans were sealed and heated/cooled with reference to an empty pan.

Compound **2a** starts to decompose at around 280 °C. The DSC curve shows an endothermic melting process (enthalpy of 18.96 J/g) which begins at 232 °C (peak at 248 °C). There is no crystallization process observable which is probably due to decomposition of the compound.

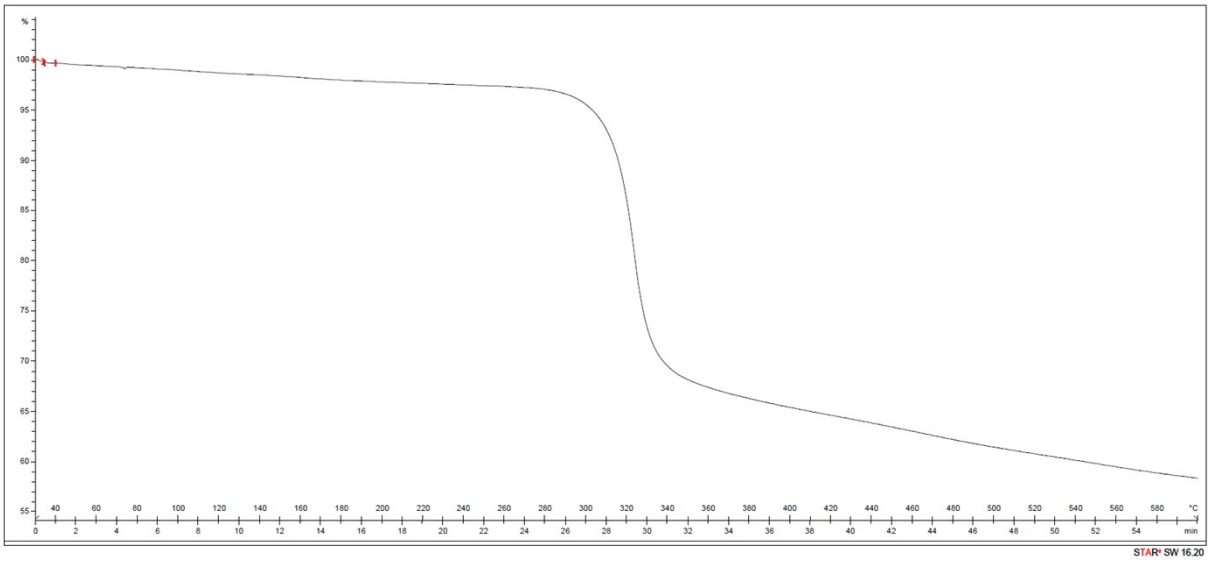

Figure S7. TGA curve of compound **2a** (3.15 mg, 30-600 °C, 20 K/min).

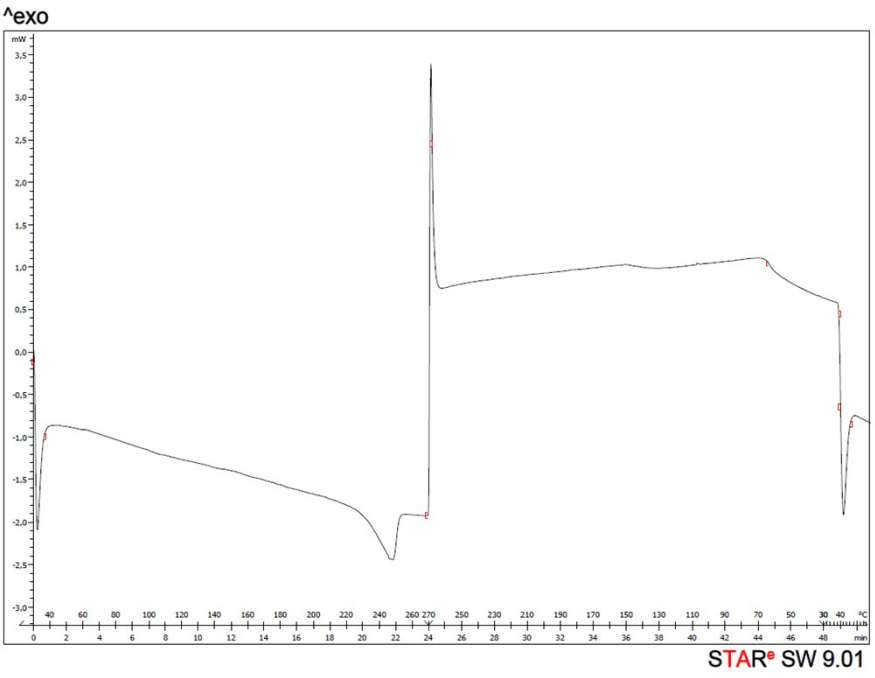

Figure S8. DSC curve of compound **2a** (2.35 mg, 30-270 °C, one cycle, 10 K/min).

Compound **2b** starts to decompose at around 300 °C. In the DSC curve from 30-300 °C are no thermodynamic processes observable.

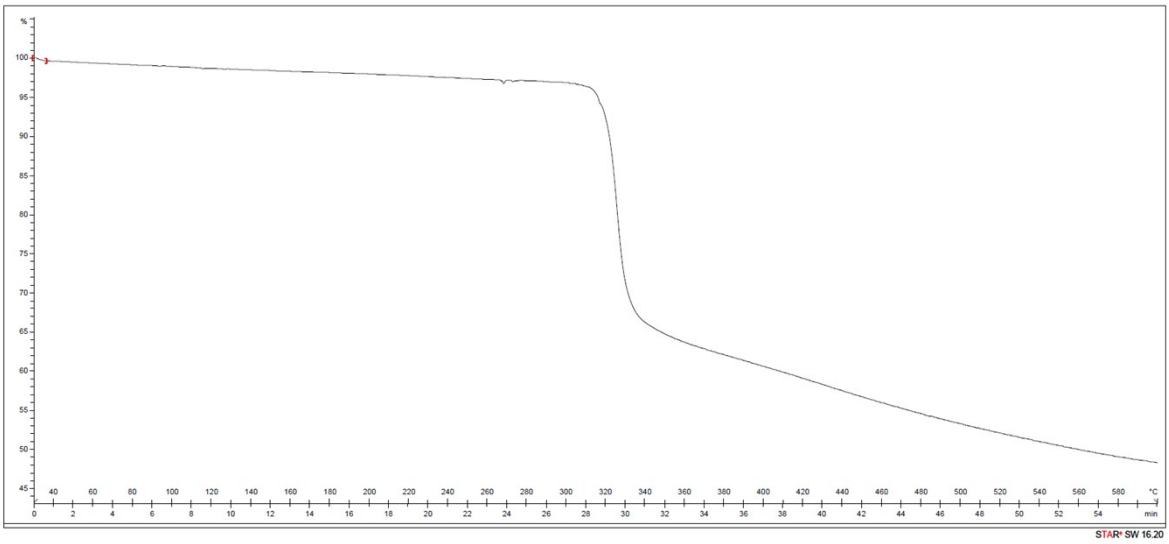

Figure S9. TGA curve of compound **2b** (1.77 mg, 30-600 °C, 20 K/min).

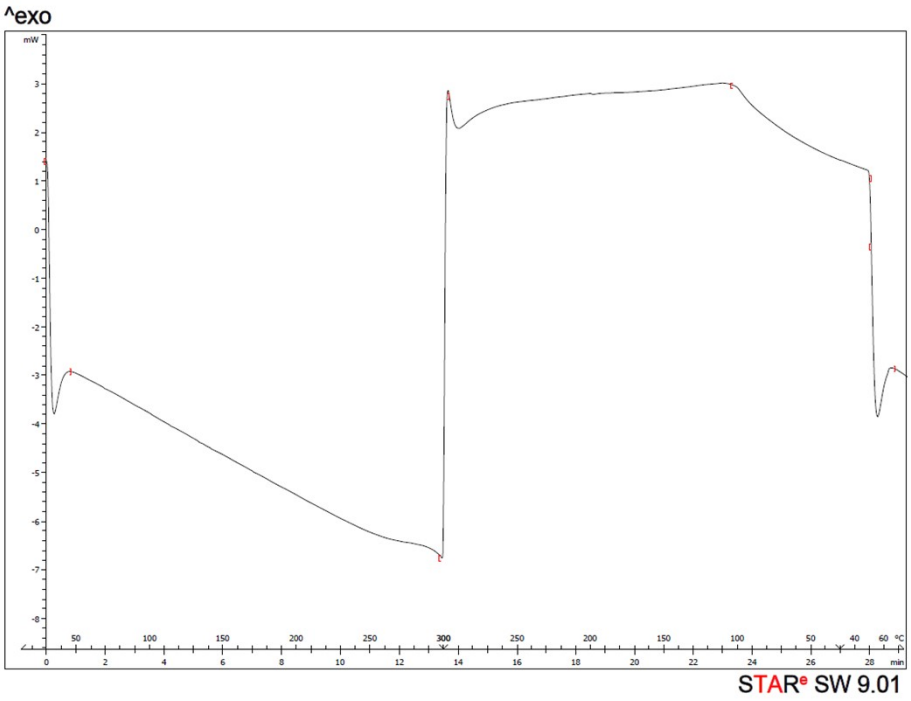

Figure S10. DSC curve of compound **2b** (4.17 mg, 30-300 °C, one cycle, 10 K/min).

TGA of compound **3a** reveals a weight loss starting at around 140 °C which could be due to dissociation of the urea substituents or a sublimation process. The compound starts to decompose completely at around 360 °C. The DSC curve shows an endothermic melting process (enthalpy of 6.65 J/g) which begins at 107 °C (peak at 117 °C). There is no crystallization process observable which is probably due to decomposition of the compound.

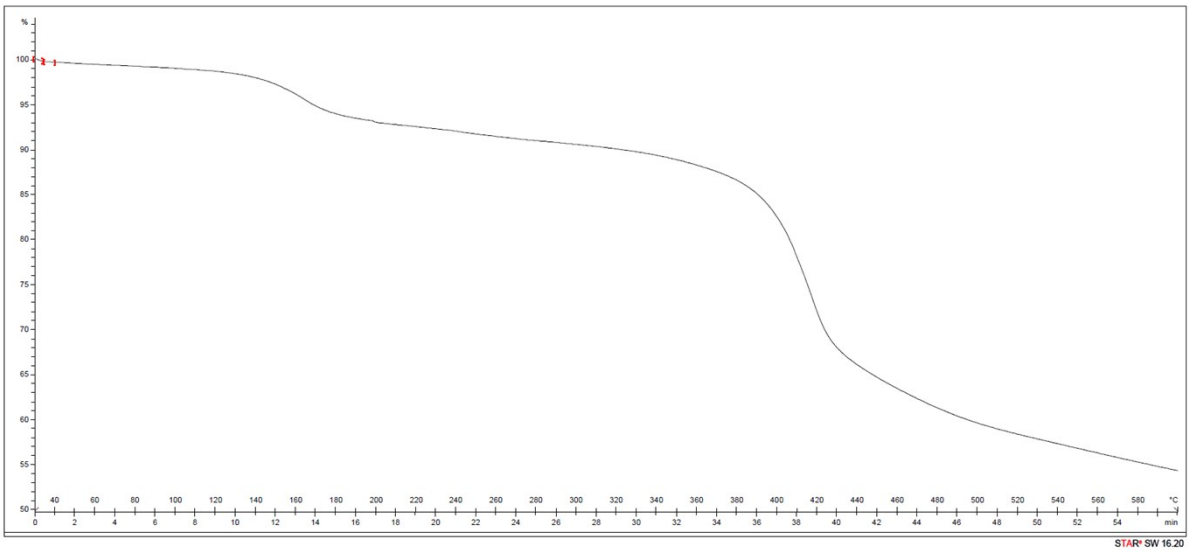

Figure S11. TGA curve of compound **3a** (3.00 mg, 30-600 °C, 20 K/min).

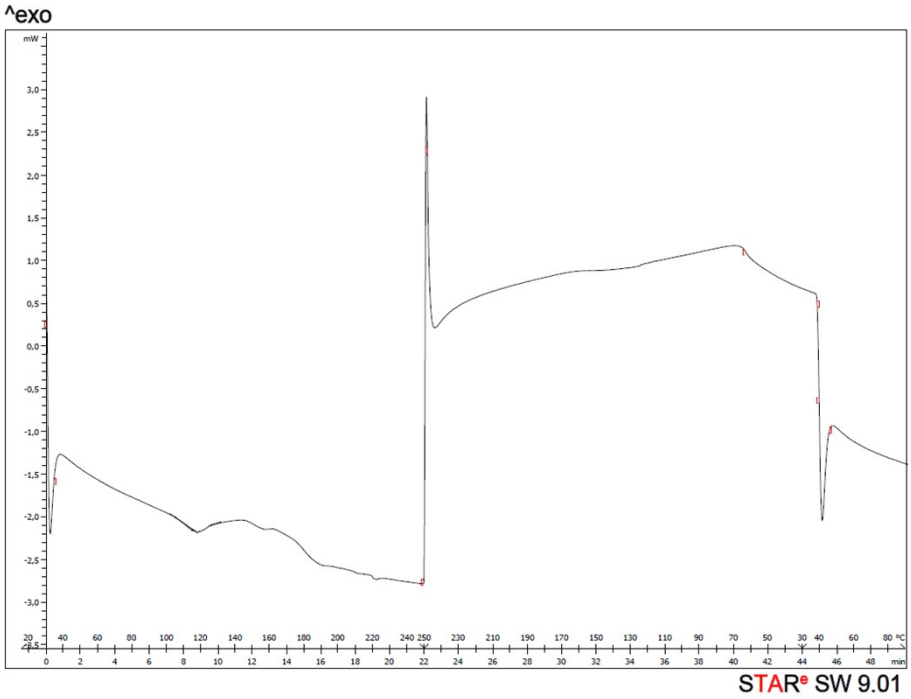

Figure S12. DSC curve of compound **3a** (2.61mg, 30-250 °C, one cycle, 10 K/min).

The decomposition of compound **3b** starts at around 340 °C. In the DSC curve from 30-280 °C there is a glass transition at 148 °C observable. The corresponding transition upon cooling occurs at 143 °C. No melting/crystallization processes are observable.

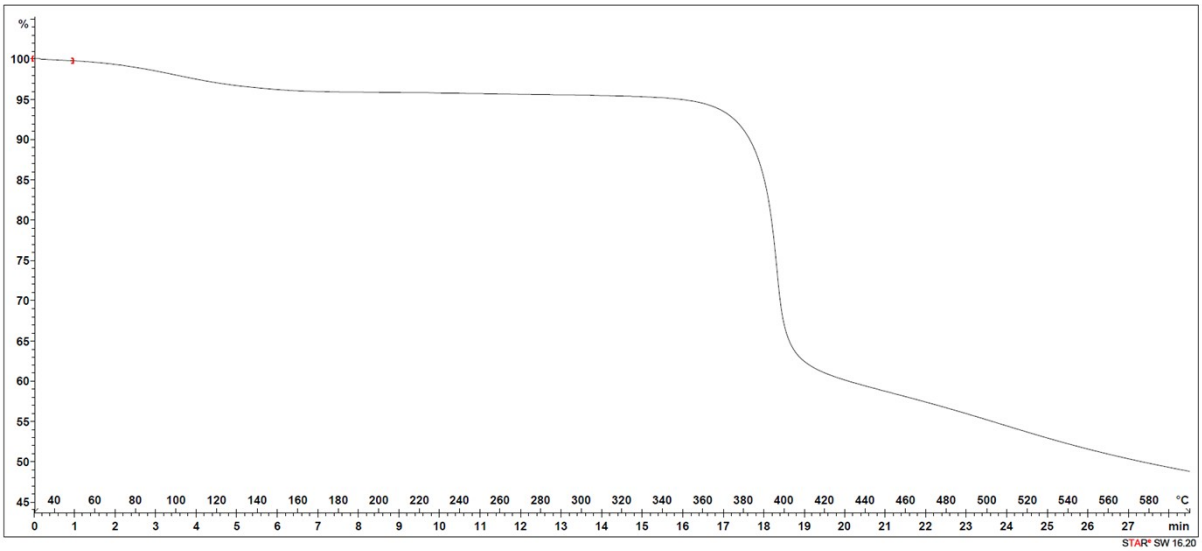

Figure S13. TGA curve of compound **3b** (7.18 mg, 30-600 °C, 20 K/min).

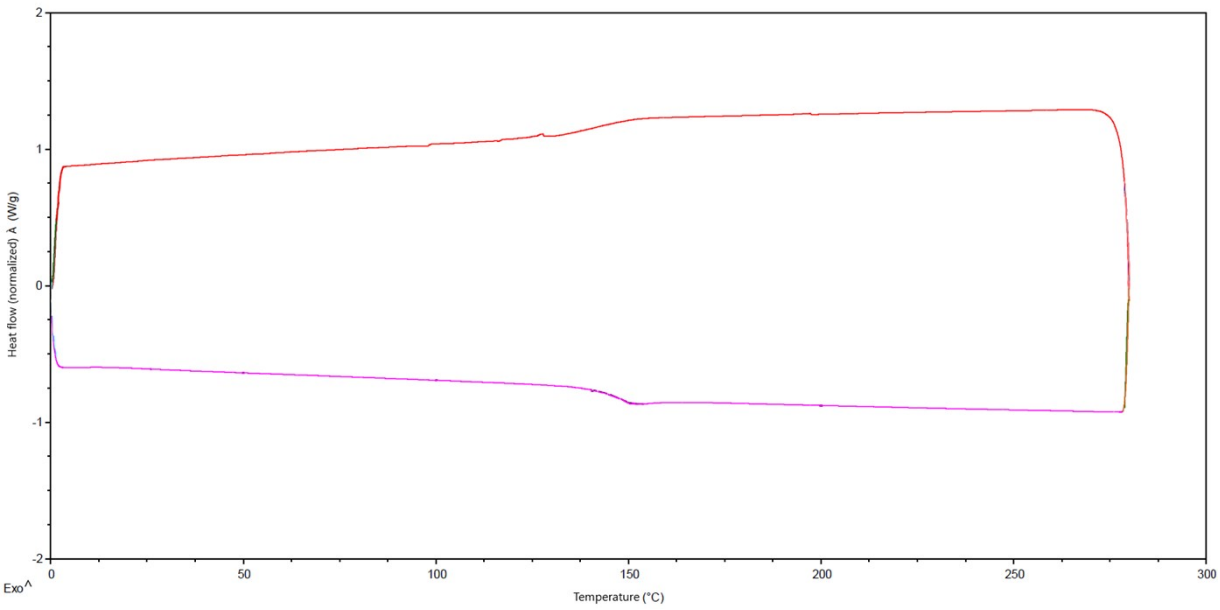

Figure S14. DSC curve of compound **3b** (5.98 mg, 30-280 °C, 1 cycle, 20 K/min).

Calculation of Fluorescence Lifetimes

Fluorescence lifetimes were calculated according to the Strickler-Berg equation:[25]

$$\frac{1}{\tau_0} = 2.88 \times 10^{-9} \eta^2 \frac{\int I(\nu) d\nu}{\int \nu^{-3} I(\nu) d\nu} \int \frac{g(\nu)}{\nu} d\nu \qquad (1)$$

(A) (B)

Absorption and emission spectra were recorded in diluted (10^{-5} M) solutions. η is the refractive index of the solvent (dichloromethane, 1.4125[26]). To obtain A two curves were plotted, one of the corrected fluorescence intensity against the frequency in wavenumbers, and the other one additionally multiplied by ν^{-3}. The ratio of the areas under the curve gives A. B was obtained by plotting the absorption spectra in molar absorption coefficients divided by the wavenumber against the wave numbers and integrated over the lowest absorption band including the vibrational shoulders.

UV/Vis Absorption and Emission Spectra of 3b

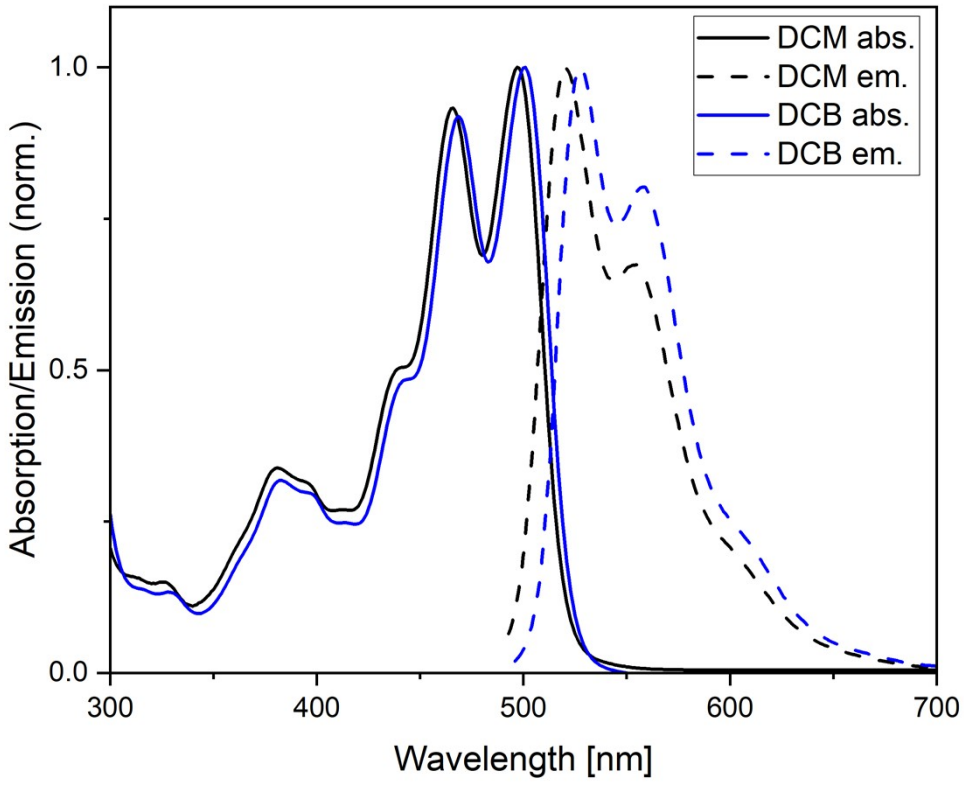

Figure S15. Absorption and emission spectra of **3b** in dichloromethane (DCM) and 1,2-dichlorobenzene (DCB, c ≈ 10−5 M, ambient temperature, excitation wavelength: 492 nm and 496 nm, respectively). Absorption maxima: 497 nm (DCM) and 501 nm (DCB); emission maxima 520 nm (DCM) and 529 nm (DCB); Stokes shifts: 889 cm^{-1} (DCM) and 1057 cm^{-1} (DCB).

Resolution Tests

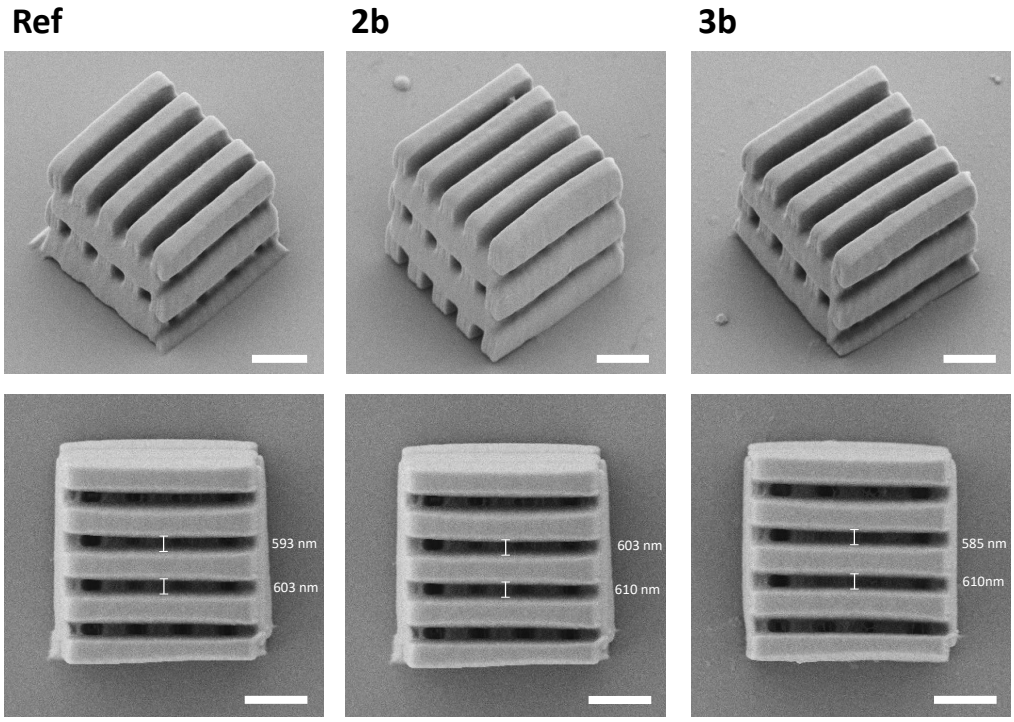

Figure S16. Woodpiles printed using the reference sample and the formulation containing the fluorophores 2b and 3b (top: titled view, down: top view). Scale bar = 2 µm

4. References

(1) G. R. Fulmer, J. M. Miller, N. H. Sherden, H. E. Gottlieb, A. Nudelman, B. M. Stoltz, J. E. Bercaw and K I. Goldberg, *Organometallics*, 2010, **29**, 2176–2179.

(2) B. M. Ferrier and N. J. Campbell, *J. Chem. Soc*., 1960, 3513-3515.

(3) T. Wesp, T. Bruckhoff, J. Petry, H. Wadepohl and L. H. Gade, *Chem. Eur. J*, 2022, **28**, e202200129.

(4) M. J. Frisch, G. W. Trucks, H. B. Schlegel, et al., Gaussian, Inc., Wallingford CT, **2016**.

(5) (*a*) C. Lee, W. Yang and R. G. Parr, *Physical Review B*, 1988, **37**, 785; (*b*) A. D. Becke, *J. Chem. Phys.*, 1993, **98**, 5648; (*c*) P. J. Stephens, F. J. Devlin, C. F. Chabalowski and M. J. Frisch, *J. Phys. Chem.*, 1994, **98**, 11623.

(6) (*a*) F. Weigend and R. Ahlrichs, *Phys. Chem. Chem. Phys.*, 2005, **7**, 3297; (*b*) F. Weigend, *Phys. Chem. Chem*. *Phys*., 2006, **8**, 1057.

(7) S. Grimme, J. Antony, S. Ehrlich and H. Krieg, *J. Chem. Phys.*, 2010, **132**, 154104.

(8) S. Grimme, S. L. Ehrlich and L. Goerigk, *J. Comput. Chem.*, 2011, **32**, 1456.

(9) (*a*) V. Barone and M. Cossi, *J. Phys. Chem. A*, 1998, **102**, 1995; (*b*) M. Cossi, N. Rega, G. Scalmani and V. Barone, *J. Comput. Chem.*, 2003, **24**, 669.

(10) (*a*) F. Neese, *Comput. Mol. Sci.* 2012, **2**, 73; (*b*) F. Neese, *Comput. Mol. Sci.*, 2018, **8**, e1327; (*c*) F. Neese, F. Wennmohs, U. Becker and C. Riplinger, *J. Chem. Phys.*, 2020, **152**, 224108.

(11) F. Neese, *J. Comp. Chem.*, 2003, **24**, 1740.

(12) F. Weigend, *Phys. Chem. Chem. Phys.,* 2006, **8**, 1057.

(13) Chemcraft: A graphical software for visualization of quantum chemistry computations. https://www.chemcraftprog.com

(14) K. Kabsch, M. G. Rossmann, E. Arnold, Eds., *International Tables for Crystallography*, Vol. *F*, Ch. 11.3, Kluwer Academic Publishers, Dordrecht, The Netherlands, 2001.

(15) CrysAlisPro, Agilent Technologies UK Ltd., Oxford, England, UK, 2011-2014 and Rigaku Oxford Diffraction, Rigaku Polska Sp. z o. o., Wrocław, Poland, 2015-2021.

(16) (*a*) SCALE3 ABSPACK, CrysAlisPro, Agilent Technologies UK Ltd., Oxford, England, UK, **2011-2014**; (*b*) Rigaku Oxford Diffraction, Rigaku Polska Sp. z o. o., Wrocław, Poland, **2015-2021**.

(17) R. H. Blessing, *Acta Cryst.*, 1995, **A51**, 33.

(18) W. R. Busing, H. A. Levy, *Acta Cryst.*, 1957, **10**, 180.

(19) O. V. Dolomanov, L. J. Bourhis, R. J. Gildea, J. A. K. Howard and H. Puschmann, *J. Appl. Cryst.*, 2009, **42**, 339.

(20) (*a*) G. M. Sheldrick, SHELXT, University of Göttingen and Bruker AXS GmbH, Karlsruhe, Germany, 2012-2018; (*b*) M. Ruf, B. C. Noll, Application Note SC-XRD 503, Bruker AXS GmbH, Karlsruhe, Germany 2014; (*c*) G. M. Sheldrick, *Acta Cryst.*, 2015, **A71**, 3.

(21) (*a*) G. M. Sheldrick, G. M., *SHELXL-20xx*, University of Göttingen and Bruker AXS GmbH, Karlsruhe, Germany 2012-2018; (*b*) G. M. Sheldrick, *Acta Cryst.*, 2008, **A64**, 112; (*c*) G. M. Sheldrick, *Acta Cryst.*, 2015, **C71**, 3.

(22) (*a*) J. S. Rollett, Eds. F. R. Ahmed, S. R. Hall and C. P. Huber, *Crystallographic Computing*, Munksgaard, Copenhagen, Denmark, p. 167, 1970; (*b*) D. Watkin, Eds. N. W. Isaaks and M. R. Taylor *Crystallographic Computing 4*, Ch. 8, IUCr and Oxford University Press, Oxford, UK, 1988; (*c*) P. Müller, R. Herbst-Irmer, A. L. Spek, T. R. Schneider, M. R. Sawaya, Ed. P. Müller, *Crystal Structure Refinement*, Ch. 5, Oxford University Press, Oxford, UK, 2006; (*d*) D. Watkin, *J. Appl. Cryst.*, 2008, **41**, 491.

(23) A. Thorn, B. Dittrich and G. M. Sheldrick, *Acta Cryst.*, 2012, **A68**, 448.

(24) (*a*) P. v. d. Sluis and A. L. Spek, *Acta Cryst.*, 1990, **A46**, 194; (*b*) A. L. Spek, *Acta Cryst.*, 2015, **C71**, 9.

(25) S. J. Strickler and R. A. Berg, *J. Chem. Phys.*, 1962, **37**, 814-822.

(26) J. E. Bertie, Z. Lan, R. N. Jones and Y. Apelblat, *Appl. Spectrosc.*, 1995, **49**, 6, 840-851.